Technologies and Processes for the Advancement of Materials

Thermal processing

ISSUE FOCUS ///

GEAR APPLICATIONS / INSPECTION & METROLOGY

MODELING LUBRICANT FLOW AND THERMAL RESPONSE FOR GEARS

COMPANY PROFILE ///

Schunk

DECEMBER 2025
thermalprocessing.com

SCR POWER CONTROLS

- 10-1200 Amps, 12-600 Volts.
- 5-Year Warranty
- 100% Amp Rating @ 50°C.
- Touch Safe Isolated Heat Sinks and SCRs
- Custom Engineered Power & Temperature Control Systems
- Fastest turnaround times: No Expediting Charges.
- Cost Effective, Competitive Pricing.
- Designed, built, assembled & tested in the USA

c UL us

CE

At Avatar Instruments, SCR power controls and systems are our main business. Not some accessory or acquisition. We understand the tough demands of industrial environments, power lines and processes. Our products are built to last decades of service.

Avatar Instruments has over 50 years of experience building with SCRs.

Contact us today to put our experience to your advantage.

302-703-6865 scrpower.com

AVATAR INSTRUMENTS

VACUUM HEAT TREATMENT SERVICE SOLUTIONS

Maximize efficiency.

- Vacuum pump solutions
- Hot zone repairs and builds
- Spare parts and maintenance kits
- Field service
- Vacuum furnace services

Trust VESCO's expert service technicians for all your vacuum furnace needs.
From repairs and reconditioning to retrofits and relocation, we keep your system running at peak performance.

Contact us today!

VESCO LLC
860-627-7015 | vacuumengineering.com

VESCO
A Company of the BUSCH Group

CONTENTS ///

COVER PHOTO: SHUTTERSTOCK

DEPARTMENTS ///

UPDATE ///

New Products, Trends, Services & Developments

Q&A ///

MICHAEL ZULAUF

PRODUCT MANAGER ///
WEILER ABRASIVES

RESOURCES ///

International Federation for Heat Treatment (IFHTSE)

The international association whose primary interest is heat treatment and surface engineering shares news of its activities to promote collaboration on issues affecting the industry. **10**

Industrial Heating Equipment Association (IHEA)

The national trade association representing the major segments of the industrial heat processing equipment industry shares news of its activities, training, and key developments in the industry. **12**

METAL URGENCY ///

A virtual inspection method for heat-treated gears to better correlate simulation results with measurements. **14**

HOT SEAT ///

Primary causes of tempered martensite embrittlement, which affects steel toughness, are cementite precipitation, impurity segregation, and retained austenite decomposition. **16**

Thermal Processing is published monthly by Media Solutions, Inc., 266D Yeager Parkway Pelham, AL 35124. Phone (205) 380-1573 Fax (205) 380-1580 International subscription rates: $105.00 per year. Postage Paid at Pelham AL and at additional mailing offices. Printed in the USA. POSTMASTER: Send address changes to *Thermal Processing* magazine, P.O. Box 1210 Pelham AL 35124. Return undeliverable Canadian addresses to P.O. Box 503 RPO West Beaver Creek Richmond Hill, ON L4B4R6.

FROM THE EDITOR ///

2025 — another year in the books

The end of 2025 is here before, it seems, it even started.

On a positive note, it looks like the heat-treat industry continues on its journey to return to normal.

So, as we enter 2026 and beyond, let this not only serve as a season's greeting, but also as a promise that *Thermal Processing* will continue to explore ways to enhance our products with the ultimate goal to getting the best and latest information about the heat-treating industry in your hands — whether that be virtually or literally — just as we did this year and in many years' past.

But before we say a final goodbye to 2025, make sure you take some time to discover this month's issue of *Thermal Processing*, which contains quite a bit of information.

December's topics are gear applications as well as metrology and inspection.

With our sister publication being *Gear Solutions*, it only makes sense that we tackle how those gears need some type of heat treating before they are able to perform their delicate, often complex, tasks.

In our cover article on gear applications, Weixue Tian, Pinzhi Liu, Michael Blumenfeld, and Ganta Naveen look at modeling lubricant flow and the thermal response for gears.

Our second feature from Wanhui Huang, Liping Lei, and Gang Fang takes a deep dive into optimizing heat treatment to improve the microstructures and mechanical properties of 5CrNiMoV steel.

Also, be sure and check out this month's company profile with Schunk and how the centery-old company has been a leading supplier in the field of carbon technology by producing customized solutions for demanding industrial applications across the globe.

You'll find that and much more in our December issue. And keep in mind that we are always looking for interesting and educational editorial content, so if you have a technical paper or other heat-treat-related articles you'd like to see published, please contact me. I'd love to hear from you and be given the opportunity to share your unique knowledge with our readers.

Happy holidays from all of us at *Thermal Processing*. Stay safe, and, as always, thanks for reading!

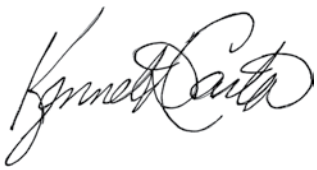

KENNETH CARTER, EDITOR
editor@thermalprocessing.com
(800) 366-2185 x204

CALL FOR ARTICLES Have a technical paper or other work with an educational angle? Let Thermal Processing publish it. Contact the editor, Kenneth Carter, at *editor@thermalprocessing.com* for how you can share your expertise with our readers.

Thermal processing

David C. Cooper
FOUNDER

Teresa Cooper
PUBLISHER

EDITORIAL

Kenneth Carter
EDITOR

Jennifer Jacobson
ASSOCIATE EDITOR

Joe Crowe
ASSOCIATE EDITOR | SOCIAL MEDIA

SALES

Glenn Raglin
VICE PRESIDENT I SALES & MARKETING

Ben Keaten
VICE PRESIDENT I SALES & MARKETING

Jared Kaplan
MEDIA CONSULTANT

Gavin Lovingood
MEDIA CONSULTANT

Morgan Butler
MEDIA CONSULTANT

DESIGN

Michele Hall
GRAPHIC DESIGNER

CONTRIBUTING WRITERS

MICHAEL BLUMENFELD
GANG FANG
WANHUI HUANG
LIPING LEI
PINZHI LIU
D. SCOTT MACKENZIE
JASON MEYER
GANTA NAVEEN
WEIXUE TIAN

media solutions

PUBLISHED BY MEDIA SOLUTIONS, INC.
P. O. BOX 1987 • PELHAM, AL 35124
(800) 366-2185 • (205) 380-1580 FAX

David C. Cooper
FOUNDER

Teresa Cooper
PRESIDENT

IHEA INDUSTRIAL HEATING EQUIPMENT ASSOCIATION

IFHTSE

THERMOCOUPLE TECHNOLOGY

CUSTOM SENSOR MANUFACTURER

Proudly Made in the USA

ACCURACY. RELIABILITY. SOLUTIONS.

PRODUCTS

- THERMOCOUPLES & RTD ASSEMBLIES
- THERMOWELLS
- PROTECTION TUBES
- THERMOCOUPLE WIRE / MULTI CABLE
- THERMOCOUPLES & RTD ACCESSORIES
- ALLOY PIPE & TUBING

SERVICES / CAPABILITIES

- ENGINEERED SOLUTIONS FOR YOUR PROCESS
- ALLOY APPLICATION ENGINEERING
- GTAW CERTIFIED TECHNICIANS
- CALIBRATION & CERTIFICATION

TTEC®

WWW.TTECONLINE.COM • SALES@TTECONLINE.COM

215-529-9394

Solar Atmospheres' new 10-bar vacuum furnace at its Greenville, South Carolina, facility will provide another regional option for high-pressure quenching of large components and workloads. (Courtesy: Solar Atmospheres)

Solar Atmospheres commissions 10-bar vacuum furnace

Solar Atmospheres announced the installation and commissioning of a new 10-bar vacuum furnace at its Greenville, South Carolina, facility.

Manufactured by sister company Solar Manufacturing, this state-of-the-art horizontal vacuum furnace features a working zone measuring 48" wide x 48" high x 96" deep and can process loads up to 12,000 pounds. The system's advanced vacuum pumping package achieves an ultimate vacuum level of $1x10^{-6}$ Torr, ensuring superior performance for processing titanium and other high-grade alloys requiring pristine vacuum environments.

"We're proud to offer our customers another regional option for high-pressure quenching of large components and workloads, while also providing the opportunity to reduce processing costs through economies of scale," said Steve Prout, president of Solar Atmospheres Southeast. "This addition reinforces our ongoing commitment to innovation, quality, and customer value."

MORE INFO www.solaratm.com

Rodney Strasser joins Ipsen USA in Southeast region

Ipsen USA has hired Rodney Strasser as the new regional service manager in the Southeast region. Operating out of Atlanta, Georgia, Strasser will be responsible for coordinating and leading a team of Ipsen service technicians who serve Ipsen customers in Delaware, Maryland, Virginia, North Carolina, South Carolina, Georgia, Tennessee, Alabama, and Florida.

Strasser joins Ipsen after 25 years working with major manufacturers developing and operating extensive service networks. A graduate of Georgia Tech, with an MBA from Georgia State University, Strasser has applied his industrial management education toward building service networks for global companies across multiple industries.

"Accepting the position at Ipsen appealed to me because I have the opportunity to make an immediate impact," said Strasser. "I've been working with capital equipment throughout my service career. Some of the experiences in my previous roles can potentially make significant and lasting improvements to the Ipsen service model."

In his first weeks at Ipsen, Strasser has focused on connecting with internal department leads who work closely with the company's customer service network across North America.

Rodney Strasser

"By supporting our efforts in the field, they provide us with the tools we need to maintain high standards in customer satisfaction with our regular customers," Strasser said. "New tools and a fresh approach can also help us improve relationships with former customers, regaining their confidence in Ipsen service."

"My goal is to grow our service revenue by expanding service agreements with more Ipsen customers, and delivering service excellence that will have a positive impact on Ipsen's market share in the industrial furnace service business," Strasser said. "Right now, I'm focused on absorbing the training resources Ipsen has made available, and building relationships with the employees that I can rely upon to assist my team of field service engineers and Ipsen's customers to achieve success."

MORE INFO www.ipsenglobal.com

SEND US YOUR NEWS Companies wishing to submit materials for inclusion in Thermal Processing's Update section should contact the editor, Kenneth Carter, at editor@thermalprocessing.com. Releases accompanied by color images will be given first consideration.

Bodycote's 55,000-square-foot heat treatment site in Fairfield, Ohio, is nearing full-scale operations with Nadcap accreditation for heat treating, vacuum brazing, and TIG welding. (Courtesy: Bodycote)

Bodycote achieves Nadcap accreditation at new Ohio facility

Bodycote, the world's leading provider of advanced heat treatment and specialist thermal processing services, has announced that its new facility in Fairfield, Ohio, has achieved Nadcap accreditation for heat treating, vacuum brazing, and TIG welding, marking a key milestone in the site's progression toward full operations.

This investment strengthens Bodycote's North American footprint and supports growing demand for high-specification thermal processing in the aerospace, defense, and industrial manufacturing sectors.

Construction of the 55,000-square-foot facility began in March 2024, with initial production trials underway since March 2025. Strategically located in Fairfield, just north of Cincinnati, the site offers proximity to key customer hubs across Ohio, Indiana, and Kentucky — enabling faster turnaround times and enhanced logistics efficiency for regional manufacturers.

With Nadcap accreditation secured, Bodycote is now entering the final stages of customer qualification and production ramp-up. The facility is equipped with a state-of-the-art braze department, vacuum furnaces, aluminum furnaces, TIG weld, FPI, and is designed to meet the most demanding performance and quality standards required in critical industries.

"This accreditation underscores our commitment to quality, consistency, and service excellence for our customers," said Heidi McNary, president, Global ADE and Surface Technology at Bodycote. "Fairfield represents a key addition to Bodycote's North American network, providing increased capacity and proximity for customers in this important industrial corridor."

The Fairfield site is now accepting customer qualifications and new production work, with full-scale operations expected by January 2026. A formal customer open house and ribbon-cutting event is planned for Q1 2026, where guests will have the opportunity to tour the facility and meet the local and corporate leadership teams.

The facility is also expected to create 10 new skilled jobs in the Fairfield region, reinforcing Bodycote's continued investment in advanced manufacturing and workforce development across the state of Ohio.

Bodycote's expansion in Fairfield continues the company's investment in world-class facilities.

MORE INFO www.bodycote.com

Ipsen Connect marks two years with upgrades

Ipsen Connect, Ipsen's integrated customer service portal, celebrates its second anniversary with several key updates designed to make it easier for customers to manage their furnaces, parts, and service needs.

The latest enhancements to Ipsen Connect include a shared shipment tracking system now available to all credentialed users, along with an expanded archive of Bills of Materials covering retrofits, rebuilds, and legacy furnace models. Together, these updates provide users with faster access to the information they need — reducing downtime and streamlining the process of identifying and ordering parts.

Launched in October 2023, Ipsen Connect offers a comprehensive suite of tools for managing parts orders, scheduling service appointments, and reviewing order status in real time. The portal also provides access to Ipsen's Knowledge Base, where customers

can find best practices, troubleshooting guidance, and expert recommendations from Ipsen's engineering and service teams.

MORE INFO www.ipsenglobal.com

Hill receives distinguished MTI Heritage Award

Bob Hill, president of Solar Atmospheres of Western PA and Michigan, received the prestigious Heritage Award — the highest honor presented by MTI — at the Metal Treating Institute (MTI) fall meeting. This award recognizes an individual's lifetime commitment and significant contributions to advancing the commercial heat-treating industry.

MORE INFO www.solaratm.com

Phillips Corporation and Delta H awarded USAF contract

Phillips Corporation, Federal Division, in partnership with Delta H® Technologies, has been awarded a significant U.S. Air Force (USAF) contract to deliver 38 dual-chamber aerospace heat-treating systems.

These heat-treating systems will enhance mission-critical aircraft maintenance capabilities at bases across the United States and overseas.

The order includes 13 Model DCAHT®-181248-1200/500-MIL units and 25 Defender Series Model DEF-DC-RH-242436/1200-CH-242436/1200 units. Deliveries are scheduled over the next year to provide the USAF with cutting-edge heat-treating capabilities for aviation-grade metals — ensuring compliance with AMS2750H and NAVAIR TO 1-1A-9 standards.

"Phillips Federal is honored to support the U.S. Air Force through this partnership," said Kelley Padham, president, Phillips Corporation, Federal Division. "Our collaboration with Delta H Technologies continues to expand the boundaries of advanced manufacturing for the Department of Defense — empowering readiness, resilience, and rapid innovation wherever our warfighters serve."

Bob Hill, president of Solar Atmospheres of Western PA and Michigan, with his daughter, Courtney, and his wife, Chris. (Courtesy: Solar Atmospheres)

"Ten years ago, the Air Force asked us to help solve a problem," said Richard Conway, director and CTO of Delta H Technologies and a U.S. Air Force veteran. "As an engineer and veteran, it became a personal mission to provide the best heat-treating solutions possible. Today, knowing the USAF relies on Delta H and Phillips Federal for this critical technology is deeply humbling."

DCAHT model features:

- Dual convection-heated chambers with certified TUS work volume 18" W × 12" H × 48" L (Class 1 uniformity).
- Lower chamber operates to 1,200°F for aluminum solution heat treating with roll-away quench tank.
- Upper chamber operates to 500°F for aluminum aging.

Defender Series model features:

- Dual TUS-certified work volumes 24" W × 24" H × 36" L.
- Convection chamber operates 200°F–1,200°F (Class 1 uniformity) with rapid cooling from 1,000°F to <200°F in under 30 minutes, enabling complete solution heat treating, annealing, and aging (T6).
- Radiant chamber operates 1,000°F–2,000°F (Class 3 uniformity) with inert gas atmosphere capability.

Based in Carroll, Ohio, Delta H Technologies, LLC is an American manufacturer of advanced heat-treating and thermal-processing furnaces for aerospace, defense, and industrial applications. The company specializes in dual-chamber and custom-engineered furnace solutions designed to meet stringent AMS2750 and NADCAP requirements.

Phillips Corporation is a global leader in manufacturing solutions and services, dedicated to advancing the metalworking industry by delivering expert knowledge, innovation, and technology. It partners with manufacturers to enhance their capabilities and productivity, fostering growth and competitive advantage.

MORE INFO www.delta-h.com or www.phillipscorp.com

Delta H® Technologies heat-treat system deliveries are scheduled over the next year to provide the USAF with cutting-edge heat-treating capabilities for aviation-grade metals. (Courtesy: Delta H® Technologies)

Ipsen elevates seven to senior field service roles

Ipsen USA has promoted seven of its field service engineers to senior field service engineer in recognition of their exceptional technical expertise, leadership, and customer service.

The newly promoted team members are Matt Hopkins, Jesse Lawrence, Larry Dahm, Glenn Hawkins, Mike Dawson, Daniel Greifemberg, and Craig Ludewig.

These promotions highlight Ipsen's commitment to developing skilled service professionals who uphold the company's standard for quality, reliability, and customer trust. Each new senior engineer brings years of hands-on experience supporting customers across the United States and around the world, ensuring that Ipsen furnaces operate safely, efficiently, and to specification.

Each new Ipsen senior engineer brings years of hands-on experience supporting customers across the United States and around the world, ensuring that Ipsen furnaces operate safely, efficiently, and to specification. (Courtesy: Ipsen USA)

"A successful field service engineer is equal parts technician, problem-solver, and customer partner," said Lu Chouraki, Ipsen's field service manager. "They bring deep technical knowledge, but also the professionalism, communication, and integrity that define Ipsen in the field. Our customers rely on them not just to fix equipment, but to build confidence in every interaction."

"Field service engineers are often the face of Ipsen for our customers," said John Dykstra, Ipsen's chief service officer. "Their expertise and dedication make a measurable difference in our customer's success. We're proud to recognize these seven individuals for frequently being recognized by our customers and their peers for their skill and dedication to service."

Together, these seven technicians represent decades of experience servicing both vacuum and atmosphere industrial heat-treating systems. From mentoring new technicians to leading complex troubleshooting and installations, their technical leadership continues to strengthen Ipsen's service capabilities worldwide.

"Their promotion raises the bar across our entire service organization," Chouraki said. "As senior FSEs, they'll continue developing others, strengthening customer relationships, and setting the standard for quality and reliability. Their leadership ensures Ipsen's reputation for excellence continues to grow."

MORE INFO www.ipsenglobal.com

MacKenzie gets 2025 George H. Bodeen Heat Treating Achievement Award

D. Scott MacKenzie recently received the 2025 George H. Bodeen Heat Treating Achievement Award. He was awarded "in recognition of his unparalleled contributions to advancing quenching technology worldwide through pioneering work in quenchant materials and modeling, and for his tireless dedication to education and training within the heat treat industry."

Dr. MacKenzie retired from Quaker Houghton in January 2025 as Quaker Houghton Research Fellow. He is also an ASM Fellow.

Established in 1996, the George H. Bodeen Heat Treating Achievement Award recognizes distinguished and significant contributions to the field of heat treating through leadership, management, or engineering development of substantial commercial impact.

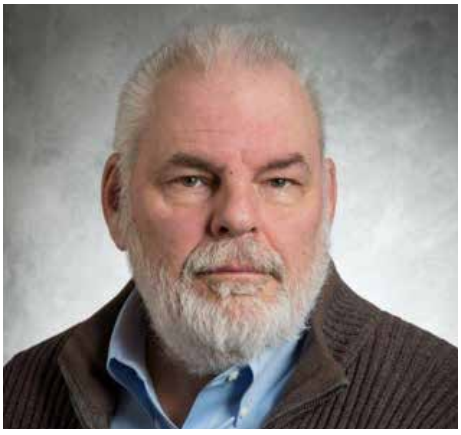

D. Scott MacKenzie received the 2025 George H. Bodeen Heat Treating Achievement Award in recognition of his contributions to advancing quenching technology and dedication to training within the heat treat industry.

HEAT TREAT 2025 WAS A SUCCESS

Heat Treat 2025, sponsored by ASM Heat Treating Society and held in conjunction with ASM IMAT, premiered in Detroit, Michigan, October 21-23 at Huntington Place. With 197 exhibitors, and more than 100 technical papers and presentations, attendance was at a record level.

CONFERENCE UPDATES

BHTS'2026
April 16-17 I Istanbul, Turkeye

BHTS'2026 – the 3rd Bosphorus International Heat Treatment Symposium will be April 16-17, 2026, at the Sabancı University Performing Arts Center in Istanbul, in collaboration with the Metal Heat Treatment Industrialists Association (MISAD) and UCTEA Chamber of Metallurgical and Materials Engineers' Training Center (METEM). The chairman of the event is Nuri Kiziltan.

Submission of final papers is January 9, 2026.

The symposium will provide a comprehensive platform to discuss heat treatment, one of the strategic fields of manufacturing, considering the latest technological and scientific developments. The goal is to bring together all stakeholders, including industry leaders, engineers, researchers, academics, and end users, to exchange knowledge, build collaborations, and shape the future of the field.

›› **For more info:** info@bhtsheat.com or www.bhtsheat.com/en

Heat Treat 2025 in Detroit, Michigan, drew 197 exhibitors and more than 100 technical papers and presentations with record attendance.

The 31st IFHTSE World Congress will be held in Cologne, Germany in 2026.

31st IFHTSE World Congress
October 13-15, 2026 I Cologne, Germany

Organized by AWT – Arbeitsgemeinschaft Wärmebehandlung + Werkstofftechnik e. V., the 31st IFHTSE World Congress will be October 13-15, 2026, in Cologne, Germany, at the International Conference and trade fair. It will include three events: HK 2026, ECHT 2026, and the 31st IHTSE World Congress

This will truly be a huge event. If you have never attended the AWT HK (H rtereiKongress) event, this is one of the largest (if not the largest) heat treating trade show in the world. This, combined with ECHT 2026 and the 31st World Congress, will be the ONE event to attend.

This large conference is organized in cooperation with the International Federation for Heat Treatment and Surface Engineering (IFHTSE) as well as the European heat treatment associations from France, Austria, Switzerland, the Czech Republic, Slovakia, and the Benelux countries. Due to the expected number of lecture registrations, the congress event is planned as a three-day event. The language of the conference will be English.

Abstracts are due March 15, 2026.

›› **More info:** www.hk-awt.de

FREE PARTICIPATION AT THE NEXT IFHTSE WORLD CONGRESS

Young researchers are invited to participate at the IFHTSE World Congress. The International Federation for Heat Treatment and Surface Engineering (IFHTSE) is dedicated to promoting the international exchange in the field. To this end, the Federation will invite some researchers younger than 35 to participate for free at the IFHTSE World Congress in Cologne in 2026. The Federation will reimburse them for the travel, accommodation, and attendance provided they present a paper in the World Congress.

Candidates shall submit:

›› A letter of support from their professor or supervisor on letterhead.

›› A summary of max 200 words on their degree program and on their present project(s).

›› A travel plan indicating the costs they expect for travel, accommodation, and registration fee.

The files can be emailed to info@awt.online.org until January 10, 2026, under the subject reference: "Free participation at the World Congress." The IFHTSE Executive Committee will then select and inform the candidates.

The candidates also should submit an abstract to www.hk-awt.de/vortragsanmeldungen by March 15, 2026.

After they have presented their papers at the World Congress the Federation, the candidate's actual costs will be reimbursed upon presentation of the tickets, invoices, etc, within the margin of the travel plan.

IFHTSE 2026 EVENTS

APRIL 16 -17
3rd Bosphorus International Heat Treatment Symposium
Sabancı University Performing Arts Center
Tuzla, Istanbul

OCTOBER 13-15
31st IFHTSE World Congress
Cologne, Germany

For details on IFHTSE events, go to www.ifhtse.org/events

IFHTSE LEADERSHIP

EXECUTIVE COMMITTEE

Prof. Massimo Pellizzari I **President**
University of Trento I Italy

Prof. Masahiro Okumiya I **Past President**
Toyota Technological Institute I Japan

Dr. Lesley Frame I **Vice President**
University of Connecticut I USA

Dr. Stefan Hock I **Secretary General**
IFHTSE I Italy

Dr. Imre Felde I **Treasurer**
Óbuda University I Hungary

OTHER MEMBERS

Prof. Rafael Colas I Universidad Autónoma de Nueva Leon I Mexico
Prof. Jianfeng Gu I Shanghai Jiao Tong University I China
Dr. Patrick Jacquot I Bodycote Belgium, France, Italy I France
Bernard Kuntzmann I Listemann AG I Switzerland
Dr. Scott Mackenzie I Quaker Houghton Inc I USA
Prof. Larisa Petrova I MADI University I Russia
Prof. Reinhold Schneider I Univ. of Appl. Sciences Upper Austria I Austria
Prof. Marcel Somers I Technical University of Denmark I Denmark
Prof. Mufu Yan I Harbin Institute of Technology I China

ONLINE www.ifhtse.org I **EMAIL** info@ifhtse.org

MEMBER SPOTLIGHT

Azbil North America offers flame safeguard equipment for combustion applications

Azbil combustion safety controllers and other products comply with international standards and support safe and reliable operation of entire facilities where combustion equipment and burners are used. (Courtesy: azbil)

As members of the IHEA heat treatment community, Azbil North America aims to make a meaningful contribution to the North American market. Being a part of IHEA will provide opportunity for new relationships and further growth in the industry. Azbil North America offers flame safeguard equipment for commercial and industrial combustion applications across the United States, Canada, and Mexico. Their product range includes burner controllers, ultraviolet flame detectors, flame relays, igniters, gas pressure switches, and more. These solutions are designed to protect employees and operations from leaks, explosions, and other thermal incidents, ensuring safety and security.

Azbil's flame safeguard and combustion control solutions provide peace of mind in various applications, such as: automotive manufacturing, commercial and captive heat treating, paint booths and ovens/paint air house units, die casting, pulp and paper mills, chemical and petrochemical industries, food and beverage processing, metal foundries, aerospace and aerostructure manufacturing, agricultural drying and preservation processing, environmental remediation, pharmaceutical plants, and the biomedical industry.

Azbil North America is actively expanding products in the mea-

Azbil product engineer Satoshi Kadoya with flame safety sensor. (Courtesy: azbil)

surement, control, and safety categories within North America's flame safety markets. Additionally, they are exploring the development of products that can contribute to carbon neutrality. Its plans include introducing products that support carbon neutrality in the furnace and oven market, contributing to both industry development, and environmental sustainability. Azbil intends to share carbon-neutral technologies — such as hydrogen and ammonia combustion — introduce suitable products and share technological advancements.

Azbil North America is headquartered in Phoenix, Arizona, and was established in 1996. Before it was known as azbil, the company started in Japan as Yamatake Shokai Co., Ltd. in 1906. After an equity-based alliance with Honeywell Inc. in 1953, it eventually became Yamatake-Honeywell. The relationship ended in 2002 but is one of the reasons many in North America immediately recognize the products. In 2008, Yamatake Corporation changed the group name to azbil Group, and as a world-class comprehensive automation manufacturer, has strived to contribute to a human-centered economy, environment, and to achieve the sustainable development of its customers and society.

Gavin DeFreese, vice president of revenue operations for Azbil North America noted they are serious about making sure its customers have the best possible flame safeguard products, but also how the people are using them in the plant.

"There are not a lot of people who understand these things anymore," he said. "Our mission is to make sure that one, people do understand the importance of these products, but two, protect those who do not and who are using and are reliant on combustion equipment for their process and operations."

The technology offered by azbil is becoming a hot topic because of workforce issues being faced globally. The setup and maintenance of combustion systems is normally performed by seasoned workers with decades of experience. As the workforce ages out, that expertise is also fading with very few young workers filling the vacancies. Azbil's products provide the much-needed safeguard, and the Azbil North America team is looking to provide better training for those products to help fill this growing experience void. Azbil provides more tools to accurately sense the preventative maintenance period. A more human-centered focus will keep them moving forward because the fundamentals of the product specs will not change.

DeFreese also pointed out an odd combination of factors that will also be part of the current heat-treating world.

"Especially with new technology, in the industrial world, you have this weird mix of 50-year-old technology and new opportunities with AI," he said. "That's one of the biggest challenges coming up in the next few years is that there are some physical safety-based systems that you will never get away from or shouldn't get away from. Sure, the information coming from these should be aggregated and used for analysis. We know how to achieve safe and stable operations and optimized maintenance through state-of-the-art technology but when it comes down to it, this is very situational based — if you have a problem, you shut down fast and safely. No compromising."

›› **For more information:** us.azbil.com

IHEA ANNUAL MEETING

Join IHEA from January 26–29, 2026, for the Annual Meeting on board Celebrity's Reflection celebrating IHEA's 97th association anniversary. For details and registration information, go to: www.ihea.org/event/AM26.

IHEA CALENDAR OF EVENTS

OCTOBER 27-DECEMBER 14

Fundamentals of Industrial Process Heating On-Line Course
Register Online at www.ihea.org

JANUARY 26-29, 2026

IHEA 2026 Annual Meeting
Location: Celebrity's Reflection cruise ship, with stops at Key West and CocoCay, Bahamas

FEBRUARY 19, 2026

Sustainability Webinar – Overview of a New US DOE Testing Platform
The new Burner Laboratories to Advance Fuel UtiliZation for Thermal Energy (BLAZE) platform is designed to accelerate the commercial adoption of fuel-flexible combustion technologies within the energy-intensive industrial heating sector.This webinar will outline how testing and developing technology within the BLAZE platform can help U.S. industries enhance energy efficiency, reduce emissions, and boost competitiveness by enabling the use of a wider range of fuels.

For details on IHEA events, go to www.ihea.org/events

JASON MEYER
MECHANICAL ENGINEER /// DANTE SOLUTIONS

A virtual inspection method for heat-treated gears to better correlate simulation results with measurements.

Bridging simulation and measurement

Gears are among the most critical and geometrically complex components in modern mechanical systems. Their performance depends not only on precise geometry but also on the precise machining of distortions caused by microstructural transformations and thermal strain that occurs during heat treatment. For decades, manufacturers have relied on physical inspection after hardening to assess how heat treatment altered the gear. However, such measurements are often costly, time-consuming, and difficult to relate to predictive simulations. A new integrated approach developed by DANTE Solutions, Inc. and Rochester Institute of Technology demonstrates how digital tools can simulate, measure, and even "virtually inspect" a heat-treated gear before it ever enters a furnace. Presented in "Integrated Heat-Treatment Simulation with Virtual Inspection of Distorted Gears" [1] at the 2023 ASM Heat Treating Society Conference, the study outlines how combining the DANTE heat-treatment simulation software with Integrated Gear Design (IGD) allows engineers to bridge the divide between thermal–mechanical modeling and shop-floor inspection. By merging simulation results with virtual metrology tools, engineers can predict distortion and evaluate common inspection metrics such as slope profile deviation, distance over balls, and base tangent length directly within the digital model. This integrated workflow effectively turns the heat-treatment simulation into a full virtual inspection process.

THE CHALLENGE: PREDICTING DISTORTION IN GEARS

Gear design involves tight tolerances and a delicate balance of geometry, material properties, and processing parameters. Standards guide designers toward suitable dimensions, but the final heat treatment can introduce distortions that shift those dimensions out of spec. Simulation tools such as DANTE have long provided insight into the stress, phase transformation, and distortion that occur during processes such as carburizing and quenching. Yet these results can sometimes be difficult to translate into the same language as coordinate measurement machine (CMM) data or shop inspection charts.

While it's easy to compare predicted changes in outer diameter or roundness, more subtle gear characteristics such as tooth thickness, slope profile deviation, and runout have been harder to visualize or quantify virtually. The challenge then remains making distortion results from heat treatment simulation measurable in the same terms as physical inspection.

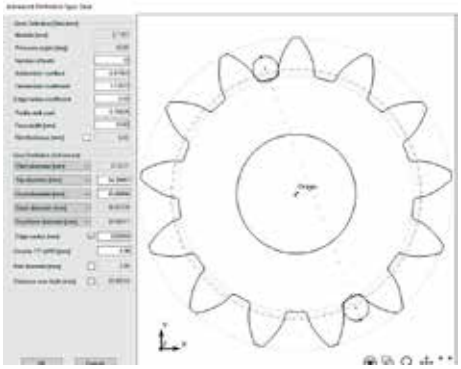

Figure 1: Pre-heat-treatment gear geometry developed in IGD.

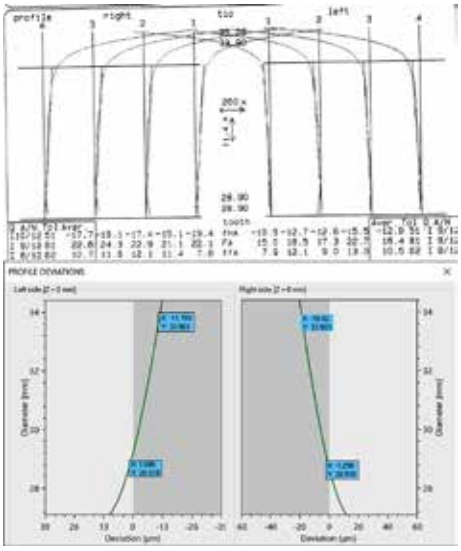

Figure 2: Measured slope profile deviations and deviations defined with IGD.

THE TOOLS: DANTE AND IGD

DANTE (Distortion ANalysis for Thermal Engineers) is a multiphase material modeling system that interfaces with major finite element solvers such as ABAQUS and ANSYS. It simulates heat-treatment processes in steels, aluminums, and nickel alloys, predicting:

- Microstructural evolution (austenite, ferrite, pearlite, bainite, martensite).
- Residual stress and distortion.
- Carburization, nitriding, and precipitation effects.
- Final hardness and phase distributions.

DANTE models capture transformations and stresses at each stage of the thermal cycle and have been widely used for process optimization, distortion minimization, and failure analysis. In this study, the predicted distortion modeling result forms the input for virtual inspection in IGD.

Integrated Gear Design (IGD) is a computer program for gear design and simulation co-developed by RIT and the Polytechnic University of Cartagena. It can generate gear geometries from manufacturing parameters, apply microgeometry modifications, perform tooth contact and finite element analysis, and automate virtual inspection of distorted geometries. IGD's standout feature is its ability to build finite element models directly compatible with DANTE. It can export meshes for heat-treatment simulation and, once the simulation is complete, import the distorted geometry back into the software. There, engineers can compare

Element	C	Mn	P	S	B
Percent	0.18 – 0.22	0.70 – 1.10	0.030 Max	0.050 Max	0.0005 – 0.0030

Table 1: Chemical composition of SAE 10B22.

the as-heat-treated gear with the nominal or finished geometry using the same measurements that would be made in a metrology lab.

CASE STUDY: VIRTUAL INSPECTION OF A CARBURIZED PINION GEAR

A combined IGD/DANTE model of a pinion gear was developed to demonstrate an example method of virtual inspection, bridging the gap between simulation results and actual gear inspection measurements. The material used in this case study is SAE 10B22, with a chemical composition shown in Table 1.

The heat-treatment process steps include gas carburizing, austenitizing, transferring to quench tank, oil quenching, and tempering. Using IGD, the pre-heat-treatment geometry is built from standard parameters such as number of teeth, diametral pitch, and base, form, and root base diameters, shown in Figure 1.

Variations in the tooth surface that influence gear noise and transmission error were also measured on four teeth and input into the pre-heat-treatment model. Figure 2 shows the measured profile deviations (fHA) with the IGD profile definitions defined; the right flank averaged 17.7 µm and the left 12.9 µm, with about a 5 µm range on each side.

IGD enables users to define these deviations directly over the gear profile, which is challenging to perform directly in most CAD platforms. Incorporating these small geometric variations before simulation ensures that the virtual twin accurately reflects real manufacturing conditions. With the gear parameters and slope definitions defined, the FEA mesh is developed for the heat-treatment model. Figure 3 illustrates IGD's mesh setup interface, where the user defines elements across the face width and tooth profile. The generated mesh and exposed surfaces are exported into an ABAQUS input format, forming the finite element model used by DANTE for thermal–mechanical simulation. The mesh in the heat-treatment model was developed with finer elements near the part surface to capture the steep thermal, chemical, and phase transformation gradients present in the heat-treatment process. The developed geometry is brought into ABAQUS and the material properties and boundary conditions, thermal and chemical, are applied for the DANTE heat-treatment model.

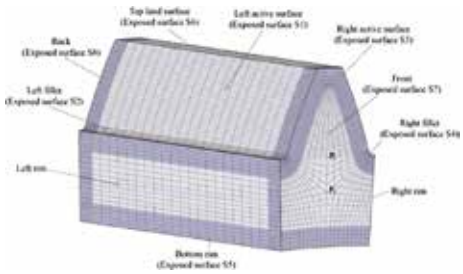

Figure 3: Developed mesh for the finite element model.

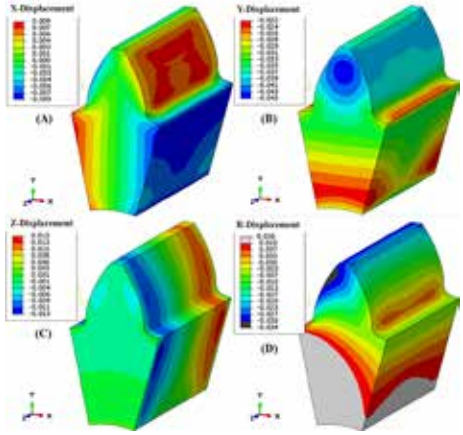

Figure 4: Distortion results for the heat-treatment model in the X direction (a), Y direction (b), Z direction (c), and cylindrical coordinates for the flank radius (d).

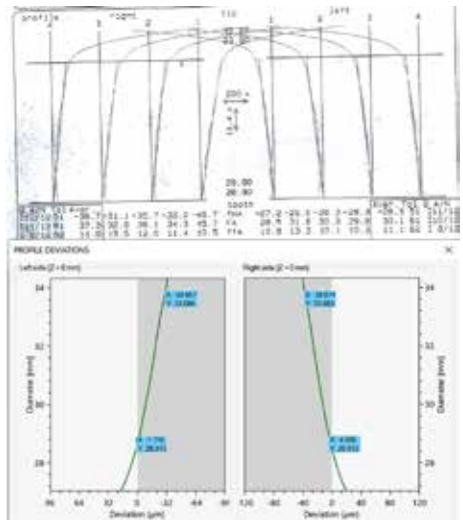

Figure 5: Measured slope profile deviations and predicted deviations measured with IGD, after heat treatment.

SIMULATION RESULTS

The DANTE model predicts several common heat-treatment results including hardness, carbon profile, phase composition, residual stress, and distortion. While hardness and stress predictions align naturally with laboratory data, distortion has been harder to validate in the same manner as a CMM would measure. The method of integrating IGD and DANTE allows the 3D displacement results to be directly compared to the measurable inspection data. Figure 4 shows DANTE's displacement predictions along the X (a), Y (b), and Z (c) axes, while Figure 4 (d) transforms these into radial coordinates. The nodes on the flank surface can be directly plotted for comparison of the flank deviations, but this would need to be automated on a case-by-case basis, which is time/cost prohibitive.

Using IGD's built-in profile deviation tool, the post-heat-treatment model is read in, and the slope profile deviations are compared to the physical measurements, Figure 5. The simulation results agree well with the measured data:

Measured (after hardening):

- Right flank: 36.7 µm average (range ≈ 15 µm)
- Left flank: 28.3 µm average (range ≈ 3 µm)

Predicted (simulation):

- Right flank: 33.9 µm
- Left flank: 28.9 µm

The virtual inspection successfully captured the direction and magnitude of distortion within experimental scatter, demonstrating the potential for quantitative process verification entirely within the virtual domain.

CONCLUSIONS

The integration of DANTE and IGD demonstrates a breakthrough in gear-process simulation. By combining DANTE's heat treat predictions with IGD's gear modeling and virtual inspection capabilities, a framework for complete digital evaluation of gears was shown. More inspection metrics can be used within IGD, such as the distance over balls, distance over pins, or the base tangent length. The ability to perform digital inspection using the same metrics as a CMM, directly from the simulation brings manufacturers one step closer to the digital twin ideal. As virtual tools grow more powerful, engineers may one day "measure" every heat-treated part before it ever leaves the computer. In that future, gear production will rely on virtual precision instead of costly trial and error.

SOURCE

[1] Sims, J., & Fuentes-Aznar, A. (2023). Integrated Heat-Treatment Simulation with Virtual Inspection of Distorted Gears. Proceedings of the 32nd ASM Heat Treating Society Conference, Detroit, MI, USA

ABOUT THE AUTHOR

Jason Meyer joined DANTE Solutions full time in May 2021 after receiving his Master's degree in mechanical engineering from Cleveland State University. His main responsibilities include marketing efforts, project work, and support and training services for the DANTE software package and the DANTE utility tools. Contact him at jason.meyer@dante-solutions.com.

D. SCOTT MACKENZIE, PH.D., FASM
SENIOR RESEARCH SCIENTIST–METALLURGY, RETIRED

Primary causes of this phenomenon, which affects steel toughness, are cementite precipitation, impurity segregation, and retained austenite decomposition.

Tempered martensite embrittlement

In this column, I will discuss tempered martensite embrittlement and its primary causes.

INTRODUCTION

Once a part has been quenched, it must be tempered. This accomplishes two things. First, it relieves the thermal and transformational stress from quenching. Second, it transforms the hard, brittle martensite to the tougher tempered martensite. For high alloy steels, it may also convert any residual retained austenite to tempered martensite or bainite.

Toughness increases as the part is tempered above 150°C. In general, as the toughness increases, the hardness decreases. For high hardness applications, the tempering temperature is kept low, usually between 150-200°C. The martensite partially decomposes and forms very fine carbide precipitates [1]. The precipitates that form are transition carbides of epsilon-carbide (ε-carbide) and eta-carbide (η-carbide) [2]. They are not cementite. There is a small increase in toughness, but the matrix remains hard.

When steels are tempered between 200-350°C, the martensite precipitates cementite (χ-carbide) and any retained austenite transform to ferrite and cementite. These carbides are coarse and occur within the plates or laths of martensite. The retained austenite begins to transform above 200°C [3]. There is a slight decrease in toughness associated with tempering in the range of 250-400°C called tempered martensite embrittlement. The typical tempering reactions in steel are summarized in Table 1.

Tempering in the temperature range of 260-370°C (500-700°F) generally causes a decrease in toughness. This is observed by a reduction in the Charpy V-Notch impact toughness or the plane-strain fracture toughness (K_{Ic}). This decrease in toughness is referred to as tempered martensite embrittlement (TME) [5]. Another type of embrittlement, called temper embrittlement (TE), may develop in steels tempered above 425°C (800°F). It is often called 350°C or 500°F embrittlement.

MECHANISM

A primary mechanism of TME involves the precipitation of cementite (Fe_3C) at prior austenite grain boundaries and interlath regions. As martensite undergoes tempering, films of retained austenite within laths partially decompose. The resulting cementite precipitates, often in the form of platelets or continuous films, act as stress concentrators and weaken local microstructure. Cementite formed in this regime is typically coarser than that produced by lower-temperature tempering, increasing susceptibility to brittle fracture [6].

A secondary mechanism involves the stability of retained austenite. As tempering progresses, retained austenite loses carbon due to cementite precipitation, becoming mechanically unstable. Under applied stress, it can transform into untempered brittle martensite. The volume change associated with the martensite transformation can contribute to cracking, or high residual stresses, especially when

Temperature Range °C		Temperature Range °F		Comments
100	200	212	390	Precipitation of transition carbides of ε-carbides and η-carbides
260	370	500	700	Transformation of retained austenite to ferrite and cementite, associated with tempered-martensite embrittlement or "blue brittleness" in low and medium carbon steels.
250	700	480	1290	Formation of ferrite and cementite
500	700	930	1290	Formation of alloy carbides of Cr, Mo, V and W. Secondary hardening occurs
350	550	660	1020	Segregation of P, Sn, Sb, As to grain boundaries resulting in temper embrittlement

Table 1: Summary of tempering reactions in steel [4].

adjacent to cementite films or prior austenite grain boundaries [7].

Certain alloying elements such as silicon or molybdenum help inhibit TME by retarding cementite precipitation and raising the critical temperature for embrittlement. Elements such as phosphorus and nitrogen tend to segregate at prior austenite grain boundaries, further reducing toughness by promoting intergranular cracking. Manganese and chromium can also play complex roles, influencing both carbide morphology and austenite stability [6] [8].

INFLUENCE OF PROCESSING PARAMETERS

The amount of embrittlement is affected by the initial microstructure, cooling rates, and tempering schedule. Oil-quenched structures with less retained austenite are less prone to severe TME than air-cooled steels with high retained austenite fractions. Rapid induction heating and cooling during tempering can suppress the formation of retained austenite, which in turn, suppresses the tempered martensite embrittlement. Prolonged tempering, even at sub-critical temperatures, can coarsen carbides and trigger TME [6].

CONCLUSION

Tempered martensite embrittlement (TME) reduces the toughness of steel when tempering in the range of 260-370°C (500-700°F). The mechanism of embrittlement is thought to be due to the formation of interlath cementite precipitation due to partial decomposition of retained austenite films. Impurity segregation such as phosphorus to prior austenite grain boundaries can aggravate the embrittlement. Alloying elements such as silicon can retard cementite formation and stabilize the retained austenite present.

Should there be any questions on this article, or suggestions for further articles, please contact the editor or the author.

REFERENCES

[1] [1] D. L. Williamson, K. Nakazawa and G. Krauss, "A Study of the Early Stages of Tempering in an 1.22%C Alloy," Met. Trans. A, vol. 10, pp. 1351-1363, 1979.

[2] [2] K. H. Jack, "Structural Transformations in the Tempering of High Carbon Martensitic Steel," ISIJ, vol. 169, pp. 26-36, 1951.

[3] [3] D. L. Williamson, R. G. Schupmann, J. P. Materkowski and G. Krauss, "Determination of Small Amounts of Austenite and Carbide in a Medium Carbon Steel by Mossbaur Spectroscopy," Met. Trans. A, vol. 10, pp. 379-382, 1979.

[4] [4] ASM International, "Introduction to Steel Heat Treatment," in Steel Heat Treating Fundamentals and Processes, vol. 4A, J. Dossett and G. E. Totten, Eds., Materials Park, OH: ASM International, 2013, pp. 3-25.

[5] [5] G. Krauss, Steels - Processing, Structure, and Performance, 2nd ed., Metals Park, OH: ASM International, 2015.

[6] [6] R. M. Horn and R. O. Ritchie, "Mechanisms of tempered martensite embrittlement in low alloy steels," Met. Trans. A, vol. 9, no. 8, pp. 1039-1053, 1978.

[7] [7] V. K. Euser, D. L. Williamson, K. O. Findley, A. J. Clarke and J. G. Speer, "The Role of Retained Austenite in Tempered Martensite Embrittlement of 4340 and 300-M Steels Investigated through Rapid Tempering," Metals, vol. 11, p. 1349, 2021.

[8] [8] H. Bhadeshia and R. Honeycombe, Steels: Microstructure and Properties, London: Butterworth-Heinemann, 2011.

ABOUT THE AUTHOR

D. Scott MacKenzie, Ph.D., FASM, Quaker Houghton Research Scientist Fellow, retired. He is the past president of IFHTSE, and a member of the executive council of IFHTSE. He can be reached at kb0fhp@gmail.com.

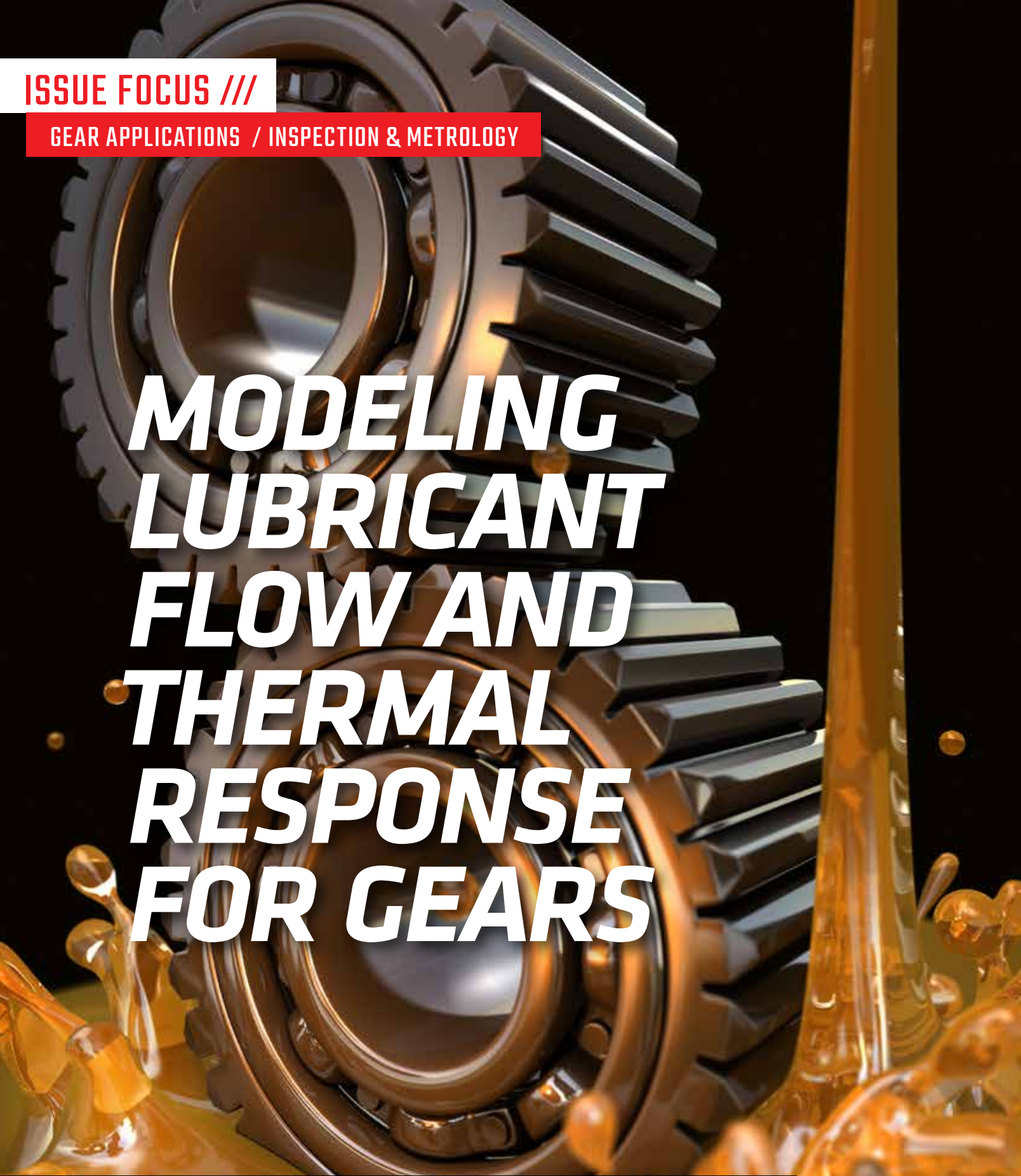

MODELING LUBRICANT FLOW AND THERMAL RESPONSE FOR GEARS

Two aspects related to gearbox lubrication are investigated: A computational fluid dynamics model for gearbox churning and the thermal response of gear bulk teeth temperature.

By WEIXUE TIAN, PINZHI LIU, MICHAEL BLUMENFELD, and GANTA NAVEEN

Interactions between gear and lubricant are very important for understanding and predicting the efficiency and durability of a gearbox. This study investigates two aspects of lubrication related to gearboxes – lubricant flow due to rotating gears, as well as the hardware thermal response due to contact friction. The first part of the article uses computational fluid dynamics (CFD) to investigate windage and churning loss of a simple gearbox. The results of this modeling provide visualization of lubricant flow and distribution inside the gearbox, as well as quantitative prediction of churning loss inside the gearbox.

With the industry need for higher efficiency while maintaining durability for gearboxes, it is very important to understand the interactions between gears and lubricants. This study developed modeling methodologies to investigate two aspects of lubrication related to gearboxes — lubricant flow due to rotating gears, as well as the gear tooth thermal response due to contact friction. The first part of the article uses computational fluid dynamics (CFD) to investigate windage and churning loss of a simple gearbox. The results of this modeling provide visualization of lubricant flow and distribution inside the gearbox, as well as quantitative prediction of the churning loss inside the gearbox. Lubricant properties affecting the churning loss are also discussed. The second part of the article presents thermal modeling results of a Mini-Traction Machine (MTM) test rig. We chose modeling MTM test rig as the foundational technology demonstration because of its wide availability for lubricant developers and ease of experimental validation for modeling. Similar modeling procedures are also applicable for actual gear contact to estimate the bulk teeth temperature for determining oil film thickness in gear contacts.

1 OIL FLOW AND CHURNING LOSS

Oil churning is one of the main power loss mechanisms inside a gearbox. High speed rotating gears can cause significant loss primarily due to the resistance of oil and air surrounding the gear. Although the power loss and visualization of oil flow inside the gearbox are often measured and observed using a transparent gearbox, where a transparent plastic case is used to replace the metal case, therefore, offering direct observation of oil flow inside a gearbox. On the other hand, a sophisticated computational fluid dynamics (CFD) model can be a great alternative where faster turnaround time and lower cost is required, especially at early design stages of the gearbox.

In this study, we developed a two-phase fluid flow model using a commercial CFD software package, ANSYS Fluent. The model domain and gear geometry are adopted from an experimental study from Ohio State University, where the oil churning power loss is measured and reported [1]. As shown in Figure 1, the gearbox contains only one spur gear, and churning loss from the oil around the gear can be simulated and predicted. The spur gear has an outside radius of 112.5 mm, width of 28.5 mm, and 67 teeth with transverse module of 3.275 mm. The box half width is 168 mm, and its total

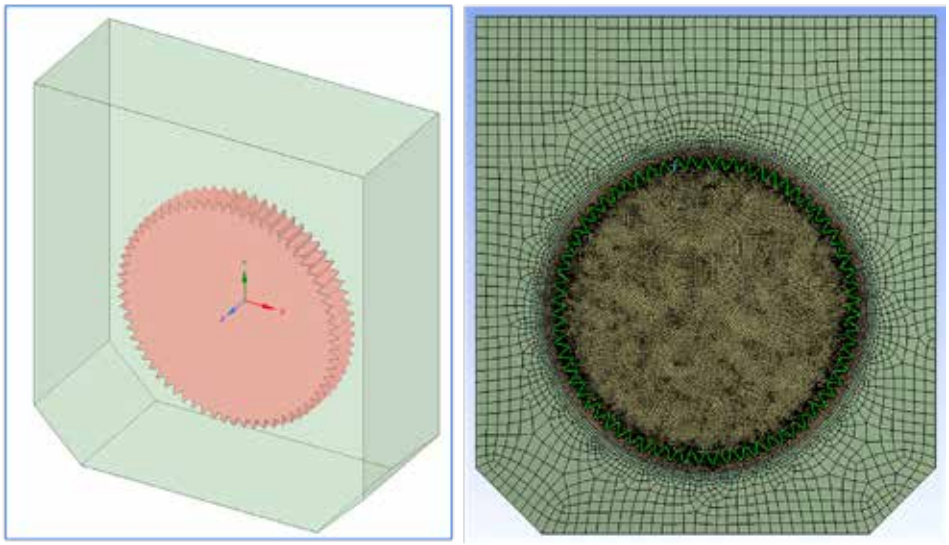

Figure 1: A simple gearbox geometry and corresponding mesh for simulation. The gear outer radius is 112.5 mm.

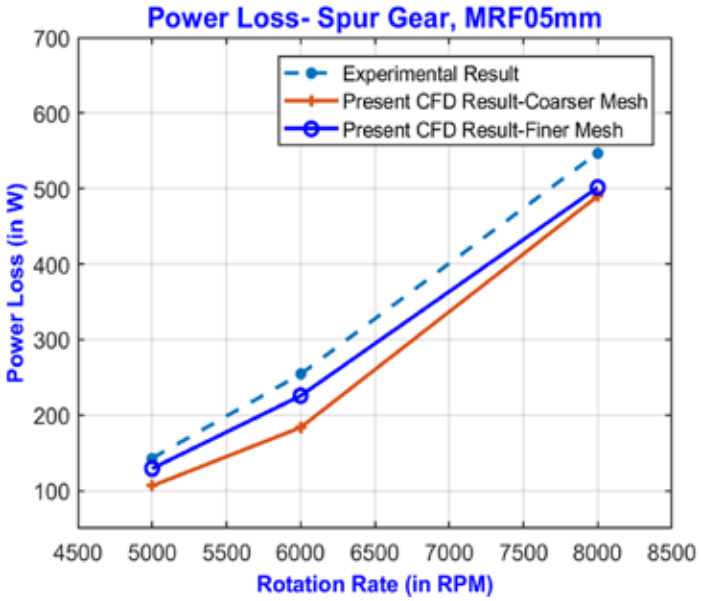

Figure 2: Comparison of windage power loss between models and tests at different rotating speeds.

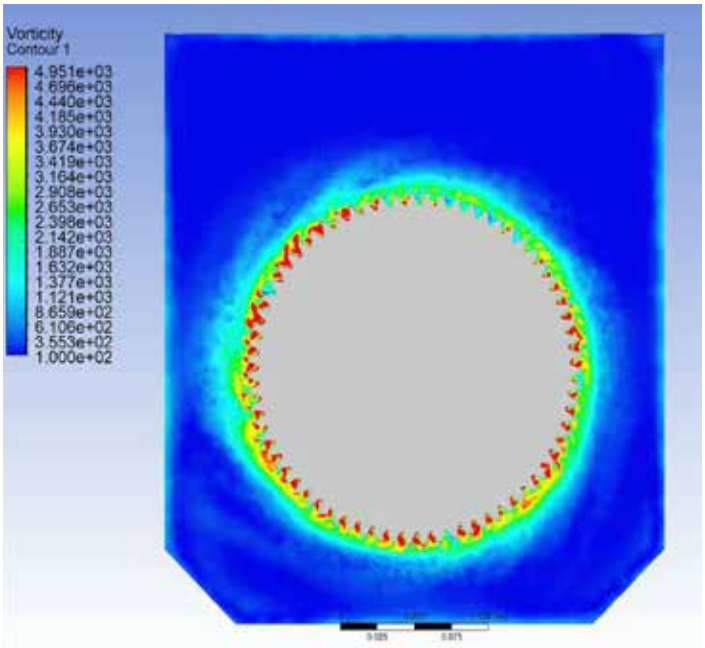

Figure 3: Vorticity contour at the mid-plane of the gear rotating at 5,000 RPM.

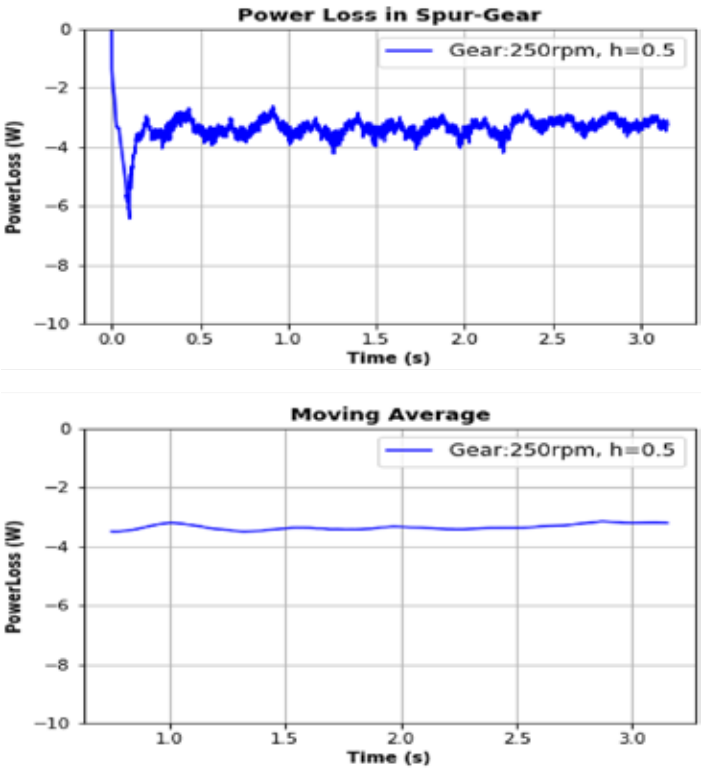

Figure 4: Reported power loss from model, top: raw data, bottom: moving average of the raw data.

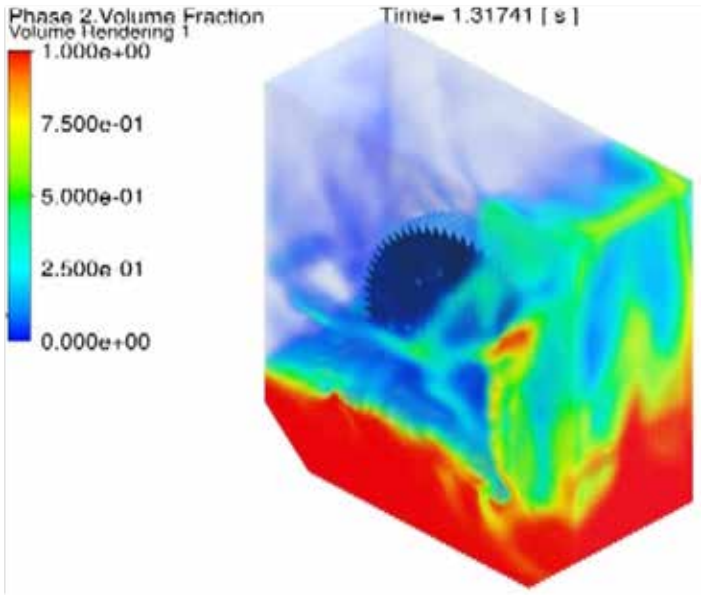

Figure 5: Volume fraction of oil in the gearbox (red color indicates high oil volume fraction).

height is 378 mm. More detailed information of the test geometry can be found in [1]. Both single phase windage loss (due to air) and two-phase churning loss (due to air and oil) are modeled and compared with experimental results. For the two-phase flow, the oil and air phases are modeled using volume of fluid (VOF) method, with air as the primary phase and oil as the secondary phase. The general methodology is widely reported in literature, e.g., [2] and is not repeated here. No slip wall boundary conditions are applied for both the gearbox and gear. No heat transfer is modeled in this investigation because the experimental results indicated that isothermal conditions were appropriate for modeling. The oil kinematic viscosity is 31.9 cSt, and density is 816 kg/m3.

A mesh sensitivity study was performed first to check the accuracy and consistency of the developed modeling procedure. In this validation study, single phase (air only) was selected for quick turnaround time. Figure 2 shows the comparison results between modeling and test. The CFD model predictions are in reasonable agreement with test results, and finer mesh appears to generate better agreement. All subsequent modeling results are based on finer mesh. The mesh sensitivity study of two-phase flow is not performed because it takes considerably more computational time. However, as seen in later discussion, the mesh employed in this article is considered sufficient as indicated by agreement between experiment and model. For single phase flow, the predicted power loss is slightly lower than the experimental results, probably due to additional frictional loss from components such as shaft and rolling element bearings, which were not modeled in this study. Figure 3 shows the vorticity contour at midplane of the gear for one of the simulated cases. The gear is rotating counterclockwise at a speed of 5,000 RPM. As expected, highest vorticity is seen close to the gear teeth due to shear flow, and the effect of the gear teeth on air flow falls off rapidly with distance away from the teeth. This indicates that the design of enclosure has limited influence on the windage power loss as long as it does not significantly affect air flow surrounding the gear.

After the modeling procedure was developed and validated, two-phase flow with different initial oil fill levels was simulated. In this simulation, the initial fill level is described by a nondimensionalized oil level height, h, defined by the oil level height from the bottom of the gearbox, divided by the distance between the bottom of the gearbox to the center of gear, e.g., h = 1 indicates the oil is filled from the bottom of the gearbox to the center of the gear. Once the gear starts to rotate, transient oil and air flow develops inside the gearbox. Continuous flow simulation shows the flow never reaches a steady state for this configuration, and the instantaneous power loss continues to fluctuate over time. The reported power loss in this article is reported as the moving average of the raw data. An example of this data processing is shown in Figure 4. The cause of the power loss fluctuation can be explained/visualized by the volume fraction

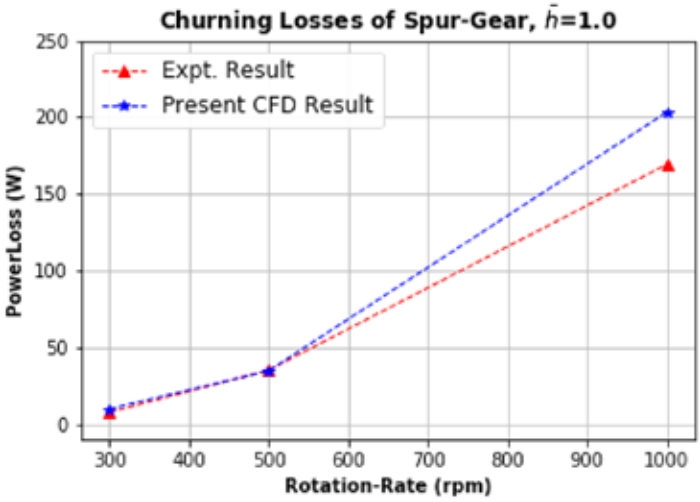

Figure 6: Churning loss comparison between experiment and model for initial oil level filled to the center of the gear.

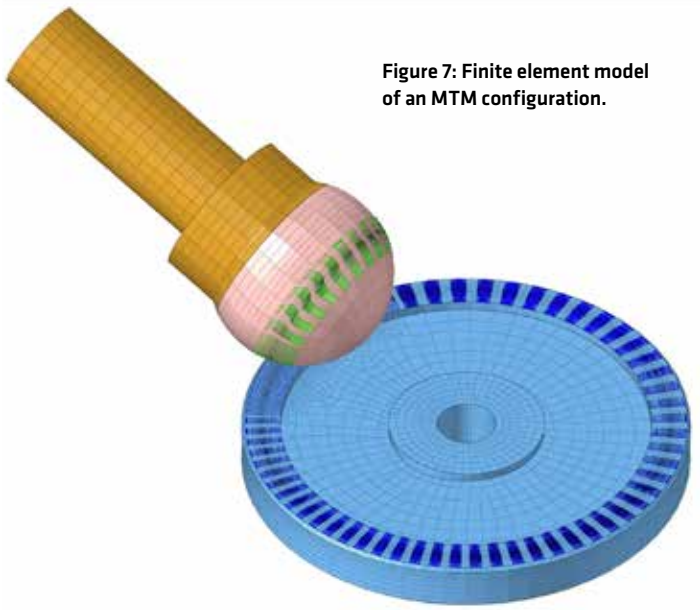

Figure 7: Finite element model of an MTM configuration.

of oil inside the gearbox, as shown in Figure 5. Oil is agitated/driven by the rotating gear, splashed to the wall, returned to sump, broken into droplet and/or mist, further splashed by the gear, and this chaotic behavior continues to evolve in the space-time domain, which generates a recurring power loss fluctuation. One example of the comparison between the CFD and experimental results is shown in Figure 6. The agreement is excellent for lower gear rotating speed. However, the discrepancy between the model and experiment increases at higher gear rotating speed. The power loss at higher gear rotating speed is probably affected by aeration/foaming of the oil, which influences the effective fill level of the oil. In addition, the wall adhesion and surface tension of the oil may also affect the returning oil flow to the sump, as well as droplet formation, therefore, changing churning power loss. More investigation is needed to examine the sensitivity of lubricant properties on the oil churning loss in the gearbox.

2 THERMAL RESPONSE OF A NON-CONFORMAL CONTACT

Gear contacts consist of a combination of sliding and rolling of the gear teeth at high pressure. During operation, temperature profiles of the gear teeth deviate significantly from ambient conditions due to frictional heating. This affects the local oil properties that have

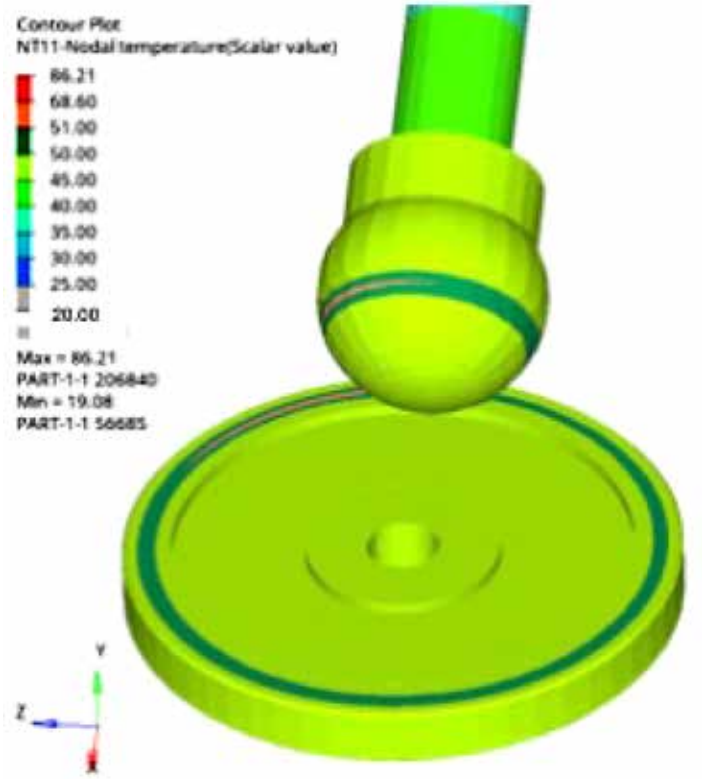

Figure 8: Typical temperature distribution for the thermal analysis.

a direct impact on the durability and efficiency of the gearbox [3]. However, measurement of the gear tooth temperature inside an operating gearbox is a significant challenge, which leads to difficulty in validating the various models for local contact temperature proposed in the literature. On the contrary, simple benchtop testing rigs, such as the Mini-Traction Machine (MTM), offer an easy to access opportunity to study thermal response of nonconformal contacts with demonstrated relevance to gear contacts. In this study, IR thermal imaging techniques were used to measure the thermal response of the ball and disc specimen temperature in an MTM test rig. This article reports some of the initial comparison of the numerical model and test results.

A thermomechanical finite-element model of the MTM (Figure 7) was built to understand the temperature increase for a non-conformal contact at defined slide-to-roll ratios (SRR) due to frictional heating. Ball-on-disk contact analysis was first run to generate the Hertzian contact profile. Based on the friction coefficient, entrainment speed, and SRR, the thermal load was calculated and applied with an initial 50/50 heat split on the disk and the ball. Abaqus user subroutine UMASFL was used to simulate the rotation of the ball and the disk to calculate its effect on heat dissipation. Convective heat coefficient was calculated using the method provided in [4]. The convective heat coefficient in the model was calculated using air as the experiment was conducted under drip lubrication. Both the ball and disc were fabricated from 52100 steel with a density of 7810 kg/m3, specific heat of 458 J/kg C, and thermal conductivity of 23.3 W/m C.

Figure 8 shows a typical temperature distribution for the thermal analysis with an initial temperature of 20°C. Heat bands can be observed following the rotational axes of the ball and the disk respectively with both parts heating up with time.

The model was run at the condition of 36.6N load (1 GPa), 3 m/s entrainment speed, and 50% SRR to compare with temperature mea-

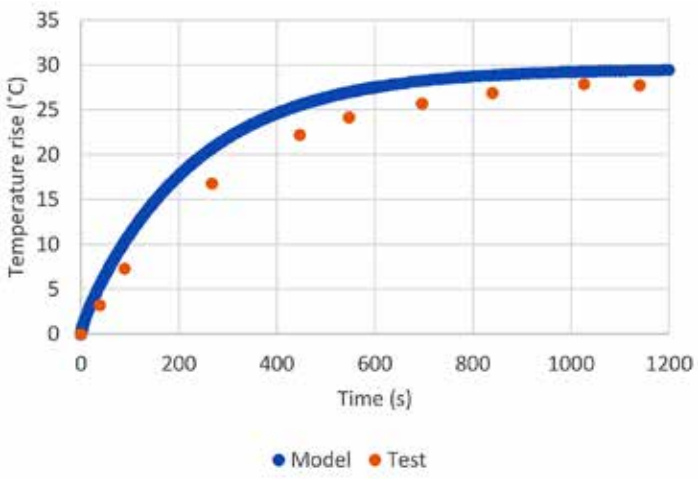

Figure 9: Temperature rise comparison between model and test for a measurement point on the disk side.

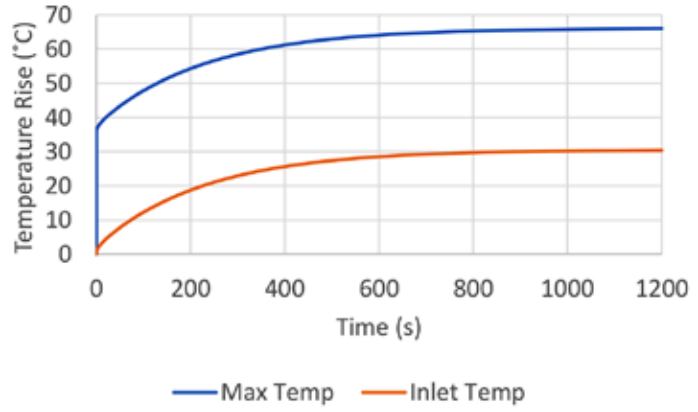

Figure 10: Model results of the max and inlet temperatures at the non-conformal contact.

surements using an infrared camera of the same MTM test of a lubricant. A mean traction coefficient of 0.0806 was applied based on the MTM test measurement. The maximum Hertzian contact pressure used in this case is not uncommon when compared to actual gear contacts, although the entrainment speed is at the lower range of typical gear contact, such as those found in various FZG gear tests. It is worth pointing out that, once the modeling procedure is developed, it is trivial to change parameters such as contact load, SRR, and entrainment speed. In addition, the effect of lubricants on thermal response, such as lower traction of Polyalphaolefin (PAO), can be modeled and predicted.

Figure 9 shows the comparison between model and experiment for the temperature rise for a single measurement point on the MTM disk. The model does a good job capturing the temperature increase over time as shown by the agreement. For this set of conditions, the disk track temperature reached equilibrium and rose by about 30°C in 20 minutes but increased by 20°C in only 5-6 minutes.

Figure 10 shows the calculated inlet and maximum temperatures of the contact at the specified conditions. Maximum temperature at the contact can be considered as a combined effect of the flash temperature and the temperature rise from the bulk. The temperature rise at the inlet will lead directly to a reduction in film thickness from the viscosity decrease of the gear oil, which can impact gear durability. Temperature rise at the contact also impacts energy efficiency and may trigger temperature-related failure mechanisms. The thermal effects during operation are critical as we balance durability vs. efficiency for gearbox designs.

3 CONCLUSIONS

Two aspects related to gearbox lubrication were investigated in this article. On gearbox churning, a computational fluid dynamics model was developed to simulate the oil flow in a simple gearbox. The churning loss of the gearbox was accurately modeled at low gear rotating speed while more discrepancy was observed at high speed. More studies are needed to understand the root cause of the discrepancy. On thermal response prediction of gear bulk teeth temperature, a model was developed for an MTM test rig and preliminary results show that the thermal response under frictional heating can be accurately predicted. The magnitude of the temperature rise identified in this study suggests that the impact of local frictional heating on oil film thickness in gear contacts is more significant than generally appreciated.

BIBLIOGRAPHY

[1] M. Handschuh, A. Guner and A. Kahraman , "An experimental investigation of windage and oil churning power losses of gears and discs," Proc IMechE Part J: J of Engineering Tribology, pp. 1-15, 2022.

[2] H. Liu, T. Jurkschat, T. Lohner and K. Stahl, "Determination of oil distribtuion and churning power loss of gearboxes by finite volume CFD method," Tribology International, vol. 109, pp. 346-354, 2017.

[3] "AGMA 925-A03, Effect of Lubrication on Gear Surface Distress," AGMA, Alexandria, VA, 2003.

[4] F. E. Kennedy, Y. Lu and I. Baker, "Contact temperatures and their influence on wear during pin-on-disk tribotesting," Tribology International, vol. 82, pp. 534-542, 2015.

ABOUT THE AUTHORS

Weixue Tian, Pinzhi Liu, and Michael Blumenfeld are with ExxonMobil Technology and Engineering Company. Ganta Naveen is with ExxonMobil Services and Technology Private Limited.

THERMAL PROCESSING MEDIA PORTAL

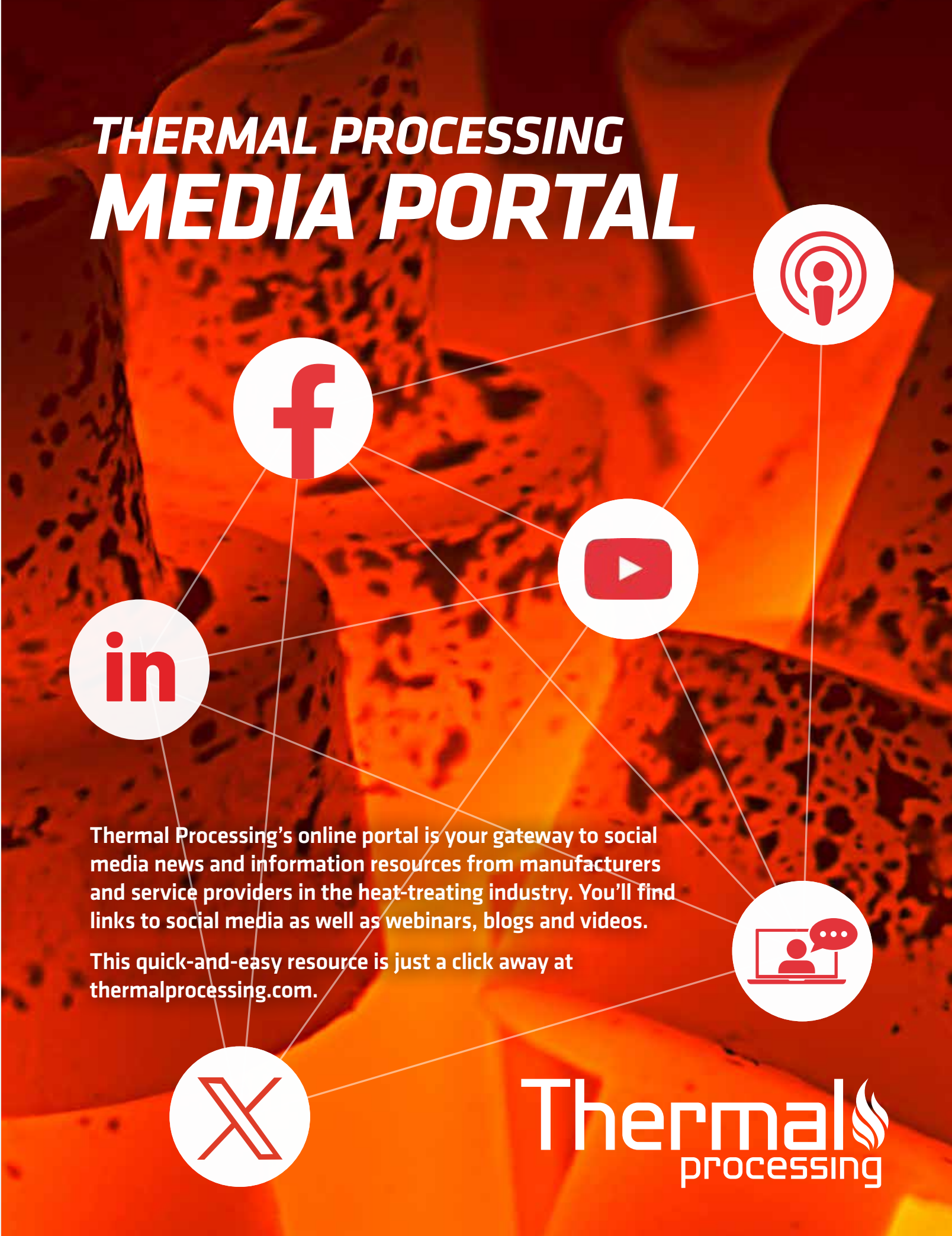

Thermal Processing's online portal is your gateway to social media news and information resources from manufacturers and service providers in the heat-treating industry. You'll find links to social media as well as webinars, blogs and videos.

This quick-and-easy resource is just a click away at thermalprocessing.com.

Thermal processing

OPTIMIZING HEAT TREATMENT

TO IMPROVE THE MICROSTRUCTURES AND MECHANICAL PROPERTIES OF 5CRNIMOV STEEL

This study reveals that, by controlling processing parameters, microstructures can be tuned to achieve comprehensive mechanical properties.

By WANHUI HUANG, LIPING LEI, and GANG FANG

A strategy combining intercritical quenching, pre-tempering, and tempering processes was implemented to optimize the microstructures and mechanical properties of 5CrNiMoV steel. By intercritically quenching at 1,050°C, pre-tempering at 600°C, and tempering at 550°C, the steel exhibited a comprehensive performance with a yield strength of 1,120 MPa, an ultimate tensile strength of 1,230 MPa, and an elongation of 8.2%. The high strength of the steel is attributed to the presence of tempered martensite and abundant secondary carbides. The favorable ductility is mainly provided by the pearlite inherited from intercritical quenching and tempering. Additionally, the precipitation of secondary carbides not only enhances precipitation strengthening, but also reduces the dislocation density and lattice strain of the matrix, thereby enhancing strength and ductility. This study offers a scheme for producing strong and ductile 5CrNiMoV steel.

1 INTRODUCTION

5CrNiMoV is a low alloy martensitic die steel that is commonly used in the manufacturing of tools for forging, extrusion, and die-casting processes [1,2]. Tools made from this steel are exposed to high pressure, friction, and multiple thermal cycles during the hot forming of materials. These harsh operating conditions often lead to a limited lifespan for tools [3,4]. Therefore, it is necessary to enhance the mechanical properties of 5CrNiMoV steel.

As is well known, the microstructure of steel and alloys plays a crucial role in determining their mechanical properties, and this is widely recognized. In the case of 5CrNiMoV steel, the microstructure typically consists of martensite and dispersed secondary carbides that are formed during the process of quenching-tempering (QT) heat treatment. It is important to note that the type, morphology, distribution, and average size of these secondary carbides significantly affect the operational lifespan and reliability of the die steel [4,5,6].

In recent years, several researchers have investigated the impact of heat treatment on the microstructure and secondary carbides of die steels, as well as its effect on their mechanical properties [7,8,9,10]. During the QT treatment, the prior austenite grain size (PAGS) and volume fraction of carbides are influenced by the quenching temperature, while the martensite morphology and secondary carbides size are influenced by the tempering temperature [7]. It has been observed that increasing the tempering temperature leads to the precipitation and coarsening of spherical carbides in the martensite lath [8]. Additionally, Zhu et al. [9] proposed the pre-tempering process can refine the tempered martensite and carbides of H13 die steel. The findings indicate that fine grains, lath martensite, and carbides contribute to the ductility and strength of H13 die steel [9,10].

Moreover, recent research has reported that steel containing a microstructure consisting of at least two distinct transformation products can attain both high strength and high ductility [11,12,13]. Sun et al. [11] demonstrated that a layered structure of martensite and ultrafine-grained ferrite can circumvent the strength-toughness trade-off typically observed in low-alloyed steel. The findings reveal that in comparison to a tempered martensitic microstructure, the martensite and ultrafine-grained ferrite layered microstructure exhibit a significant enhancement in impact toughness. Furthermore, He et al. [12] and Li et al. [13] successfully developed medium-manganese steels featuring a refined austenite and martensite structure. This advanced medium-manganese steel boasts an ultimate tensile strength exceeding 2,000 MPa and an elongation surpassing 20%.

Element	C	Si	Mn	Cr	Ni	Mo	V	P	S
wt.%	0.54	0.25	0.72	0.96	1.58	0.36	0.074	0.012	0.003

Table 1: Chemical compositions of the 5CrNiMoV steel (wt.%).

Gaining a comprehensive understanding of the microstructural evolution of 5CrNiMoV steel is of paramount importance. However, limited efforts have been made to elucidate the methodology for controlling the tempered martensitic microstructure in 5CrNiMoV steel. Consequently, this study aims to propose an optimal heat-treatment route to enhance its microstructures and mechanical properties. An intercritical quenching process — followed by high-temperature pre-tempering and low-temperature tempering — is developed. Furthermore, employing optical microscope (OM) and scanning electron microscope (SEM) observations, along with X-ray diffraction (XRD) and energy-dispersive spectroscopy (EDS) analyses, the microstructure evolution and precipitation behavior of secondary carbides during the heat treatment of 5CrNiMoV steel are thoroughly examined and discussed.

2 MATERIALS AND METHODS

2.1 Materials

Table 1 lists the chemical compositions of the 5CrNiMoV die steel, which was taken from an as-forged billet.

Phase transformation temperatures of the 5CrNiMoV steel were investigated using differential scanning calorimetry (DSC) measurements (STA 449F3 Jupiter). During the measurement, the specimen was heated from 25°C to 1,100°C at a rate of 10°C/s, and the heat flow rate to the specimen was monitored. In addition, a quenching and deformation dilatometer (DIL 805, TA instruments, New Castle, Delaware) was used to carry out the thermal expansion tests of the steel. The specimens used for the thermal expansion test are 10 mm in height and 4 mm in diameter. During the test, the specimens were heated to 950°C, 1,050°C, and 1,100°C, respectively, at a heating rate of 10°C/s, kept for 5 min, and then cooled at a linear rate of 50°C/s. The results of the dilatometer tests show that the Ms temperature is 240°C and the Mf is lower than room temperature.

2.2 Heat Treatment Process

Firstly, the specimens were heated to either 1,050°C or 1,100°C and held at these temperatures for 30 min. Subsequently, they were

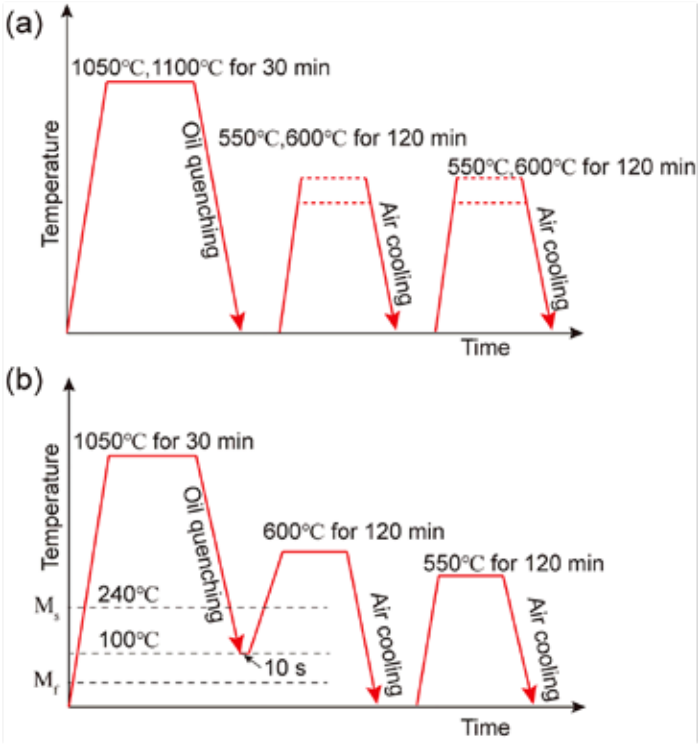

Figure 1: Schematic diagrams of heat treatments: (a) quenching and tempering, (b) intercritical quenching and tempering.

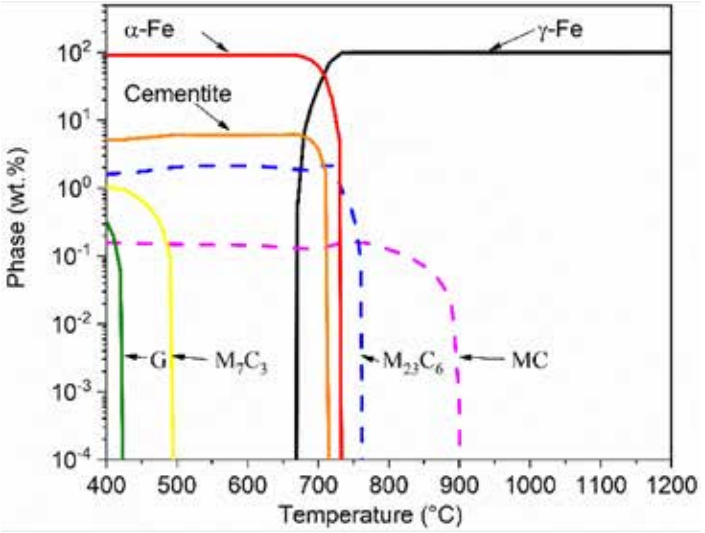

Figure 2: Equilibrium phase diagram of the 5CrNiMoV steel (calculated using JMatPro V. 7.0 software).

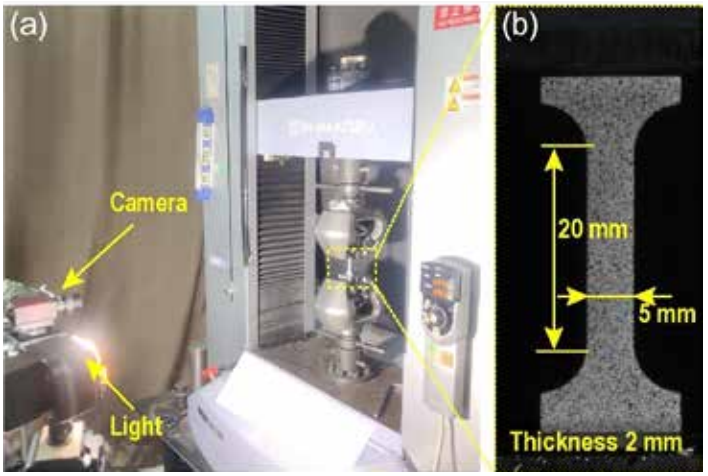

Figure 3: (a) Tensile testing equipment; (b) dimensions of the tensile specimen.

quenched in oil, as shown in Figure 1a. After the quenching process, the specimens underwent pre-tempering and tempering treatments. In the pre-tempering stage, the specimen was reheated to a temperature of either 550 or 600°C and held for 120 min, followed by air cooling. Subsequently, the specimen was reheated to a temperature that was equal to or lower than the pre-tempering temperature (550 or 600°C). Then, an intercritical quenching method was proposed to produce a mixed structure of pearlite and martensite in the 5CrNiMoV steel. This method involves quenching the specimen after isothermal holding at 1,050°C for 30 min. The quenching process was performed by rapidly immersing the specimen into a quenching oil at a temperature of about 100°C for a duration of 10 s. Subsequently, the intercritically quenched specimen underwent pre-tempering and tempering treatments, as shown in Figure 1b.

Additionally, the strength of 5CrNiMoV steel is influenced by precipitation strengthening, which is caused by the formation of secondary carbides. To determine the appropriate tempering conditions, the researchers referred to the equilibrium phase diagram of the 5CrNiMoV steel, as depicted in Figure 2. It was observed that, due to the low silicon content, the formation of cementite is more favorable compared to other carbides [14]. However, in terms of contributing to the strength of the die steel, the carbides MC and $M_{23}C_6$ play a more significant role than cementite. Based on the information provided in Figure 2, it was found that the carbides $M_{23}C_6$ and MC remain stable within the temperature range of 550°C to 650°C. Therefore, for this research, the tempering temperature was selected from a range of 550°C to 600°C.

2.3 Microstructure and Mechanical Properties Characterization

The experimental setup for the tensile tests and the dimensions of the tensile specimens are shown in Figure 3. Two tensile specimens were prepared for each heat-treated sample. The tensile tests were conducted at room temperature using a material testing machine (Shimadzu AGX-V) with a loading rate of 0.005 mm/s. To accurately measure the strain of the tensile specimen, the digital image correlation method was employed [15]. The resolution of the camera was 300 1000 = 300,000 pixels. The hardness of the quenched specimens was tested using a Rockwell hardness tester (HRS-150).

The microstructures of the specimens were examined using an OM (Zeiss, Jena, Germany, Axio Observer Z1M) and an SEM (Zeiss, Sigma 300) equipped with an EDS system. Prior to observations, all specimens were mechanically polished, ground, and subsequently chemically etched using 4% nital. Furthermore, the micro-strain and dislocation of the heat-treated specimens were estimated by the XRD (Bruker, Billerica, MA, USA, D8 Discover). The size and volume fraction of carbides were measured using Image-Pro Plus software.

3 RESULTS AND DISCUSSION

3.1 Dissolution of Carbides

As shown in Figure 4a, the transformation temperatures of Ac1 (750°C) and Ac3 (770°C) of the 5CrNiMoV steel were determined according to the heating dilatation curve. The DSC curve, shown in Figure 4b, exhibits two endothermic valleys. Previous studies have reported the transformation of ferrite to austenite, carbide dissolution, and grain growth are all endothermic processes [16,17]. Therefore, the first endothermic valley in the DSC curve corresponds to the austenite

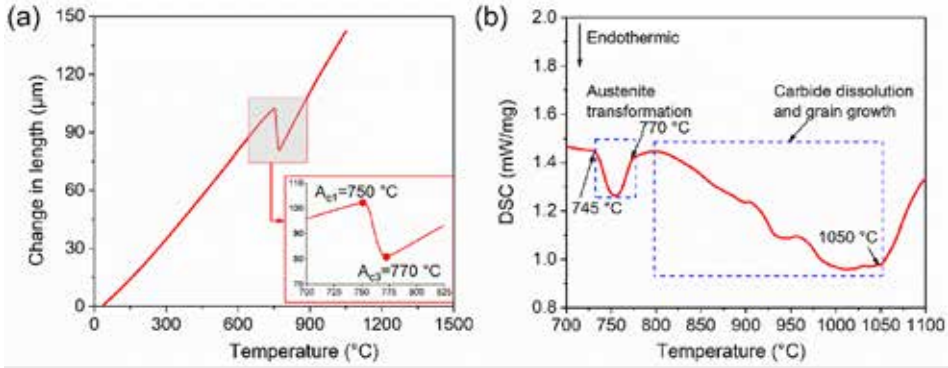

Figure 4: Transformation temperatures test. (a) The dilatometry curve and (b) the DSC curve of the 5CrNiMoV steel.

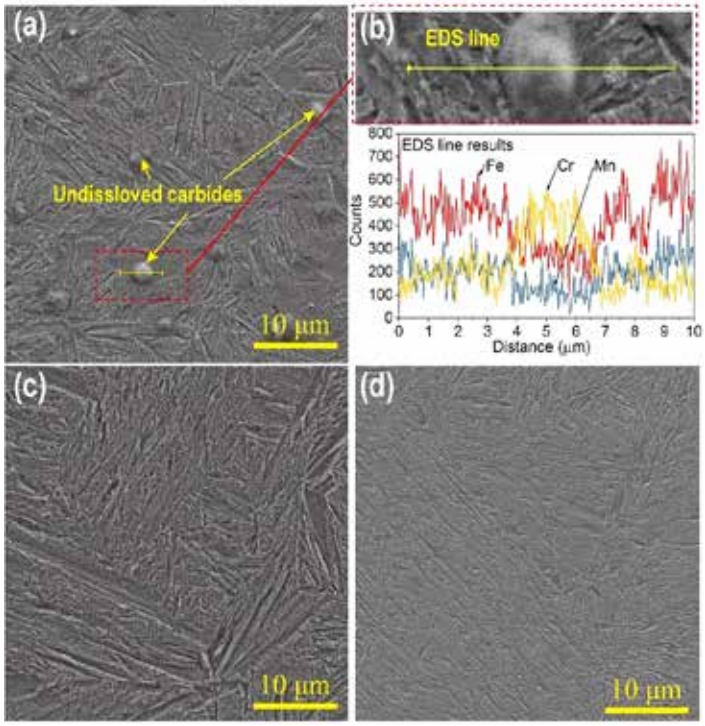

Figure 5: SEM micrographs of the 5CrNiMoV steel quenched at (a) 950°C, (c) 1,050°C, and (d) 1,100°C. (b) EDS line results of the particle in (a).

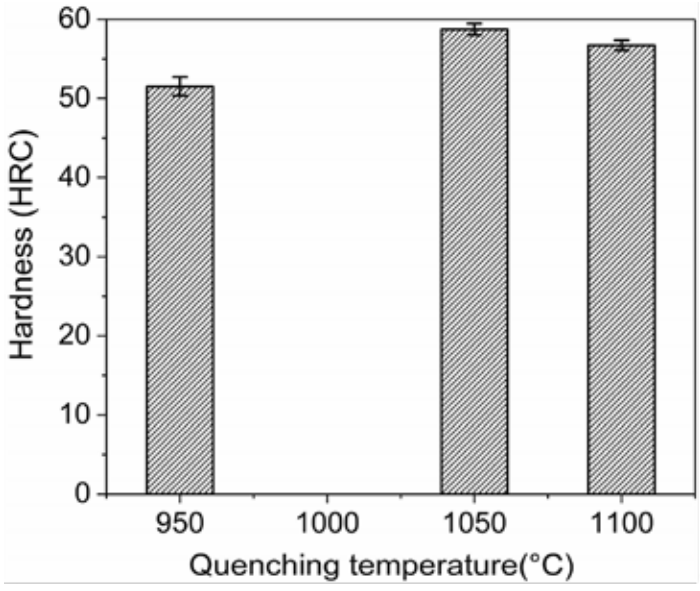

Figure 6: Martensitic hardness of the 5CrNiMoV steel quenched at different temperatures

transformation, while the second one corresponds to the grain growth and dissolution of carbides.

It is worth noting the DSC curve does not exhibit an exothermic reaction until the temperature reaches approximately 1,050°C. This suggests the complete dissolution of carbides only occurs when the temperature reaches 1,050°C.

Figure 5 displays the martensite of specimens quenched at various temperatures. As illustrated in Figure 5a, undissolved particles can be observed on the martensite matrix of the specimen quenched at 950°C, as indicated by the yellow arrows. To further investigate these particles, the chemical element variations along the line crossing them were characterized using EDS, as shown in Figure 5b. The results reveal the undissolved particle is a chromium (Cr)-rich carbide. In contrast, no such undissolved particles are observed in Figure 5c,d for specimens quenched at 1,050°C and 1,100°C, respectively.

The presence of undissolved Cr-rich carbide reduces the chromium content in the matrix structure, leading to an inhomogeneous microstructure. This inhomogeneity is detrimental to the strength of steel. As depicted in Figure 6, the specimen quenched at 950°C exhibits the lowest hardness, measuring at (52 ± 1) HRC. This decrease in hardness is attributed to the undissolved carbides (Figure 5a), which reduce the alloying elements within the quenching martensite, consequently resulting in a decrease in martensitic hardness. Upon quenching at 1,050°C, the martensitic hardness reaches its peak, measuring at (59 ± 1) HRC. However, when quenched at 1,100°C, the hardness declines to (57 ± 1) HRC. This reduction in hardness is associated with excessive quenching temperature, which leads to the coarsening of prior austenite grains and subsequently decreases the hardness of the specimen. The results indicate the presence of undissolved Cr-rich carbides in specimens quenched at lower temperatures results in an inhomogeneous microstructure and a decrease in hardness. Conversely, excessive quenching temperature causes prior austenite grain coarsening and a subsequent decline in hardness. Therefore, a quenching temperature of 1,050°C is considered reasonable for 5CrNiMoV steel.

3.2 Mechanical Properties

The engineering stress — strain curves of the heat-treated specimens are depicted in Figure 7. Furthermore, the ultimate tensile strength (UTS), yield strength (YS), and elongation to rupture (EL) of various specimens are provided in Table 2. The numbers in the legend denote the conditions of heat treatment. For instance, 1050-550-550 signifies that the quenching, pre-tempering, and tempering temperatures are 1,050°C, 550°C, and 550°C, respectively. Moreover, 1050L-600-550 indicates the implementation of intercritical quenching, where the specimen was intercritically quenched at 1,050°C, followed by pre-tempering at 600°C and tempering at 550°C.

Specimen (S) 1050-550-550 demonstrates superior strength and ductility compared to S1100-550-550. It is observed that, with an increase in quenching temperature, the UTS and YS decline from 1,375 MPa to 1,330 MPa and 1,290 MPa to 1,200 MPa, respectively. Simultaneously, the EL decreases from 4.0% to 3.0%. This can be attributed to two factors. Firstly, the PAGS and martensite block size augment with an increase in quenching temperature, thereby diminishing the YS of the quenched steel as per the Hall–Petch relation [18]. Secondly, the coarsened grains of the prior austenite and martensite blocks are susceptible to initiating micro-cracks during tensile tests, leading to

intergranular fracture, and consequently reducing the EL [19,20].

Upon comparing S1050-550-550 and S1050-600-600, it is evident that, as the pre-tempering and tempering temperatures increase, the EL also increases. Concurrently, the UTS and YS decreased significantly. This is linked to the aggregation and coarsening of the secondary carbides and decomposition of the tempered martensite induced by elevated tempering temperatures. Despite S1050-600-600 possessing high EL, the low YS severely hampers the application of the 5CrNiMoV steel.

Tempering is an effective method to modify precipitation behavior for enhancing the mechanical properties of die steels. By modulating the tempering conditions, S1050-600-550 exhibits exceptional mechanical properties, with an UTS of 1230 MPa, YS of 1120 MPa, and EL of 7.0%. Additionally, based on the aforementioned optimized parameters, the EL is further ameliorated with intercritical quenching. As delineated in Table 2, S1050L-600-550 boasts the highest EL of 8.2%, with an UTS of 1220 MPa and YS of 1110 MPa, showing better mechanical properties and can meet diverse engineering requirements.

3.3 Microstructures

Figure 8 illustrates the OM and SEM micrographs of S1100-550-550 and S1050-550-550, which have been quenched at varying temperatures. The microstructure is comprised of ferrite, tempered martensite, and secondary carbides. As shown in Figure 8a,b, a small amount of ferrite is distributed along the austenite grain boundaries, which is an important reference substance to measure the PAGS. Post-measurement, the PAGS of the specimens quenched at 1,050°C and 1,100°C are (156 ± 8) μm and (188 ± 16) μm, respectively. The migration ability of grain boundaries is enhanced at higher temperatures, thereby promoting grain growth. Consequently, the PAGS of S1100-550-550 is larger than that of S1050-550-550. During tempering, grain boundaries become the preferred nucleation sites for carbide precipitation [20]. Figure 8c,d reveals the tempered martensite is composed of martensitic lath and secondary carbides. The secondary carbide size of S1050-550-550 is small (Figure 8c). Figure 8d demonstrates that, with the rise in quenching temperature, the lath structure becomes more distinct due to the PAGS increase. Film-like carbides precipitate along the lath boundaries, forming numerous hard boundaries between the tempered martensite laths. Given the hardness of the tempered martensite matrix is inferior to that of secondary carbides, the stress concentration at the lath boundaries intensifies during tensile deformation [21]. It causes micro-cracks to form and propagate along the lath boundaries, resulting in the swift fracture of S1100-550-550. Hence, the EL of S1100-550-550 is exceedingly low.

Figure 9 presents OM and SEM micrographs of S1050-600-600 and S1050-600-550, which have been tempered at different temperatures. Owing to the identical quenching temperatures, the average diameters of PAGBs of S1050-600-600 and S1050-600-550 are closely similar: (161 ± 10) μm and (165 ± 7) μm, respectively (Figure 9a,b). However, the morphology and average size of the secondary carbides vary with the tempering temperature. Figure 9c shows when both the pre-tempering and tempering temperatures are 600°C, the secondary carbides noticeably aggregated and coarse. Additionally, the decomposition of tempered martensite laths is also clearly observed. These factors contribute to a decline in the YS of S1050-600-600, which is 670 MPa. Figure 9d indicates that, with a reduction in tempering temperature, the secondary carbide size significantly decreases. Furthermore, secondary carbides are observed not only along lath boundaries but also within martensitic laths. This suggests pre-tempering at 600°C promotes the precipitation nucleation of carbides. Subsequent tempering at 550°C not only continues to promote precipitation, but also inhibits the coarsening of the carbides. Therefore, S1050-600-550 exhibits a favorable combination of ductility and strength (Figure 7).

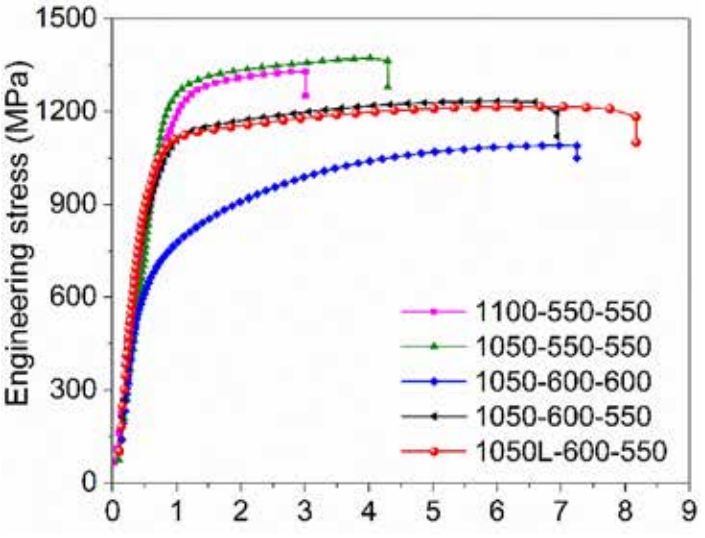

Figure 7: Engineering stress-strain curves of different heat-treated specimens.

Specimen	UTS (MPa)	YS (MPa)	EL (%)
1100-550-550	1330 ± 15	1200 ± 15 3.0	0.5
1050-550-550	1375 ± 25	1290 ± 12 4.0	0.8
1050-600-600	1090 ± 10	670 ± 8 7.0	0.6
1050-600-550	1230 ± 20	1120 ± 10 7.0	0.5
1050L-600-550	1220 ± 16	1110 ± 10 8.2	0.3

Table 2: Tensile properties of the 5CrNiMoV steel heat-treated under different conditions.

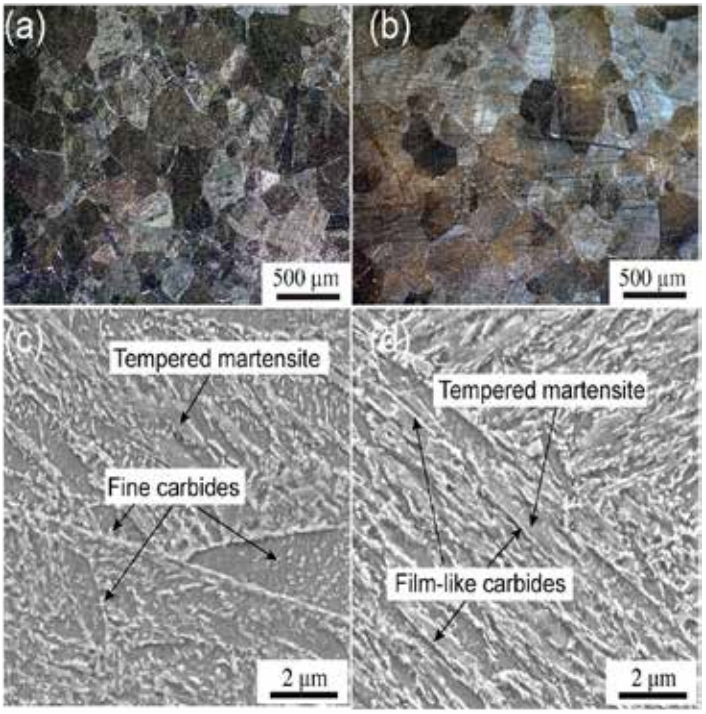

Figure 8: OM and SEM micrographs of the 5CrNiMoV steel. (a,c) S1050-550-550, and (b,d) S1100-550-550.

Figure 10 displays OM and SEM micrographs of S1050L-600-550, which underwent intercritical quenching at 1,050°C, pre-tempering

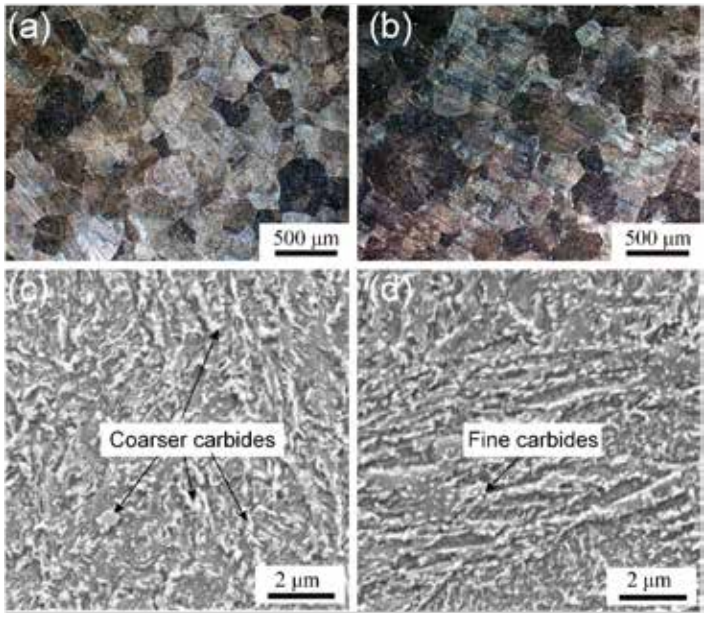

Figure 9: OM and SEM micrographs of the 5CrNiMoV steel. (a,c) S1050-600-600, and (b,d) S1050-600-550.

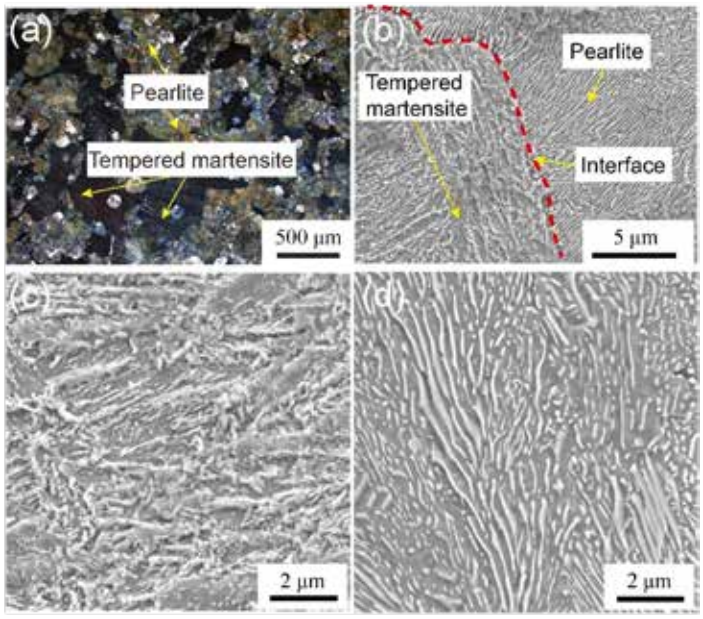

Figure 10: OM and SEM micrographs of S1050L-600-550. (a) Martensite and pearlite, (b) tempered martensite/pearlite interface, and detail of (c) tempered martensite, and (d) pearlite.

at 600°C, and subsequent tempering at 550°C. Figure 10a reveals the microstructure of S1050L-600-500 consists of tempered martensite and pearlite. Due to intercritical quenching, only a portion of austenite is transformed into martensite, while the remainder is converted into pearlite during the subsequent tempering process. Figure 10b illustrates the interface of the tempered martensite and pearlite. The detailed structures of the tempered martensite and pearlite are shown in Figure 10c,d.

Figure 11 aims to quantitatively analyze the secondary carbides in 5CrNiMoV steel by counting the volume fraction and average size. As indicated in Figure 11a,b, S1050-600-550 achieves not only a high-volume fraction (26%) of the precipitated carbides, but also suppresses carbide coarsening ((0.12 ± 0.03) μm). Regarding other specimens, S1050-550-550 has the smallest average size of the secondary carbides, which is (0.09 ± 0.02) μm. However, the lower tempering temperature is not conducive to carbide precipitation. Thus, in S1050-550-550, the volume fraction of the secondary carbides is merely 11%. In S1100-550-550, the precipitation of a large number of strip-like carbides leads to an increase in both the average size and volume fraction of the secondary carbides. In S1050-600-600, the coarsened secondary carbides are caused by a higher tempering temperature, which is detrimental to the mechanical properties of die steel and should be avoided.

3.4 Precipitation Strengthening

Due to the interaction of carbides and dislocations, precipitation strengthening is mainly related to the average size and volume fraction of the secondary carbides, which are important strengthening mechanisms of die steels [22]. According to the Ashby-Orowan model, the contribution to the YS ($\Delta\sigma_p$) of the secondary carbides is proportional to the 1/2 power of the volume fraction (f_p) and inversely proportional to the average size (d_p) of the secondary carbides [23]. It indicates that fine precipitates with fine grain size and high-volume fraction are beneficial for improving the contribution of precipitation strengthening to the YS of the 5CrNiMoV steel. The calculation formula of precipitation strengthening according to the Ashby-Orowan model is written in Equation 1 [23,24]:

$$\Delta\sigma_p = \frac{0.538Gbf_p^{\frac{1}{2}}}{d_p}\ln\left(\frac{d_p}{2b}\right) \quad \text{Equation 1}$$

where $\Delta\sigma_p$ is the contribution of YS caused by precipitation strengthening, G is the shear modulus of 5CrNiMoV steel (80.26 GPa),

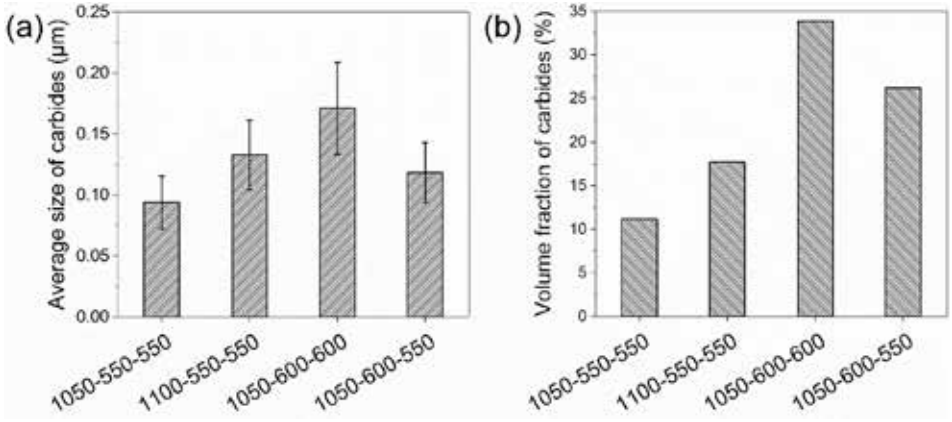

Figure 11: (a) Average size and (b) volume fraction of the secondary carbides.

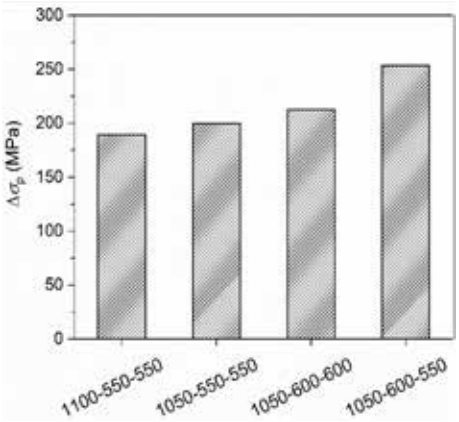

Figure 12: Contributions of precipitation strengthening to yield strength.

f_p is the volume fraction of the precipitated carbides, d_p is the average size of the precipitated carbides, and b is the Burgers vector.

Based on the information provided in Figure 11 regarding the volume fraction and average size of the secondary carbides, we have calculated the contribution of precipitation strengthening to the YS of different heat-treated specimens. Figure 12 illustrates the contribution of precipitation strengthening to YS ranges from 190 MPa to 255 MPa. Among the specimens, S1050-600-550 exhibits the highest precipitation strengthening contribution, reaching 255 MPa. This finding is consistent with the observations made on the microstructure. Specimen 1050-600-550 possesses a higher volume fraction of secondary carbides and has a relatively fine carbide size, which results in a favorable combination of strength and ductility.

Figure 13 shows the XRD pattern of the heat-treated specimens. The results show all the specimens are primarily composed of ferrite and martensite phases, and no obvious residual austenite peak is detected in the diffraction pattern.

In the XRD analysis, the instrumental broadening has been corrected with the standard broadening data of polycrystalline Al_2O_3. The crystallite size and lattice strain affect the Bragg peak width. They are important parameters to determine mechanical properties. In the ferrite phase with BCC structure, the relationship between the lattice constant (a), the Miller indices ({h k l}), and the plane spacing (d) is shown in Equation 2 [25].

$$\frac{1}{d^2} = \frac{h^2 + k^2 + l^2}{a^2} \qquad \text{Equation 2}$$

According to Bragg's law $\lambda = 2d\sin(\theta)$ and Equation 2, the value of a is calculated in Equation 3:

$$a = \frac{\lambda\sqrt{h^2 + k^2 + k^2}}{2\sin(\theta)} \qquad \text{Equation 3}$$

where θ is the Bragg angle and λ is the X-ray wavelength.

As shown in Figure 14, the average values of the lattice constant for the heat-treated specimens range from 2.8669 to 2.8681Å. Notably, the lattice constant value exhibits an inverse relationship with the volume fraction of the secondary carbides. This observation is consistent with the information presented in Figure 11b and Figure 14, where it is evident a higher volume fraction of secondary carbides corresponds to a smaller lattice constant. The increase in the volume fraction of secondary carbides with a decrease in the lattice constant can be attributed to the reduction in the content of solid solution alloying elements within the α-Fe matrix. As the volume fraction of secondary carbides increases, the amount of solid solution alloying elements decreases, leading to a reduction in lattice distortion. Consequently, the lattice constant decreases accordingly. In the case of S1050L-600-550, it undergoes intercritical quenching and tempering treatment, resulting in the formation of microstructures consisting of tempered martensite and pearlite. This specific heat-treatment process promotes the precipitation of a significant number of carbides, leading to a smaller lattice constant.

After obtaining the lattice constant, the average crystallite size is calculated using the Debye–Scherrer equation seen in Equation 4 [26].

$$D = \frac{K\lambda}{\beta\cos\theta} \qquad \text{Equation 4}$$

where θ is the Bragg angle, λ (0.154 nm) is the X-ray wavelength, β is the full width at half maximum (FWHM), and K is a constant equal to 0.89.

In addition, the lattice strain (ε) is determined according to the Williamson-Hall method [26,27]. Therefore, according to the results average crystallite size and lattice strain, the dislocation density

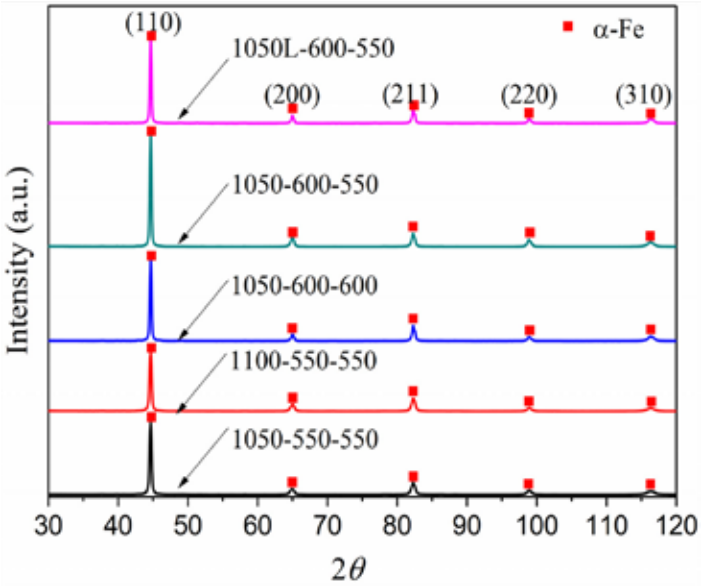

Figure 13: XRD patterns of the heat-treated specimens.

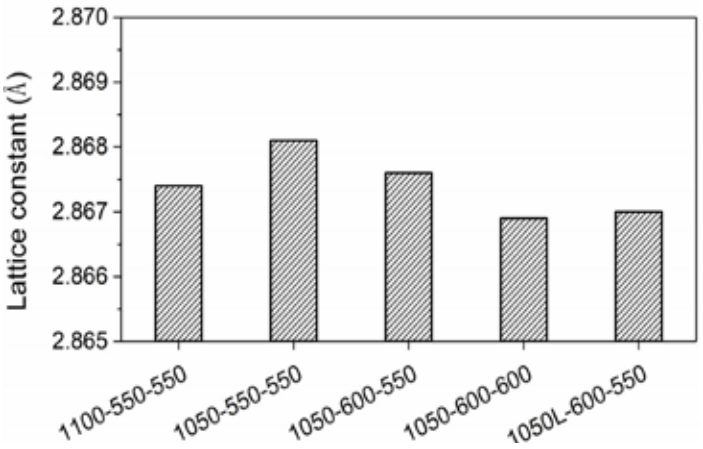

Figure 14. Lattice constant of the heat-treated specimens.

is calculated using the Equation 5 [28,29,30,31].

$$\rho = \frac{2\sqrt{3}\varepsilon}{Db} \qquad \text{Equation 5}$$

where ρ is the dislocation density, b is the Burgers vector — which for BCC metals, b =(√3/2)a — and a is the lattice constant as shown in Figure 14.

Figure 15 enumerates the computed values of the crystallite size, lattice strain, and dislocation density for all heat-treated specimens. The findings suggest these parameters are significantly influenced by the pre-tempering temperature rather than the quenching temperatures. As shown in Figure 15a, the crystallite size increases with an increase in the pre-tempering temperature, while the lattice strain decreases. This reduction in lattice strain subsequently leads to a decrease in the dislocation density within the martensite matrix (Figure 15b,c). Furthermore, there is a negligible difference in the lattice strain, crystallite size, and dislocation density between S1050-600-550 and S1050-600-600. This observation demonstrates these parameters are predominantly influenced by the pre-tempering temperature. As shown in Figure 11b and Figure 15, a higher pre-tempering temperature promotes the precipitation of carbides, thereby diminishing the lattice strain and dislocation density of the matrix, which is beneficial for enhancing the ductility of the 5CrNiMoV steel. Additionally, tempering following the pre-tempering process further

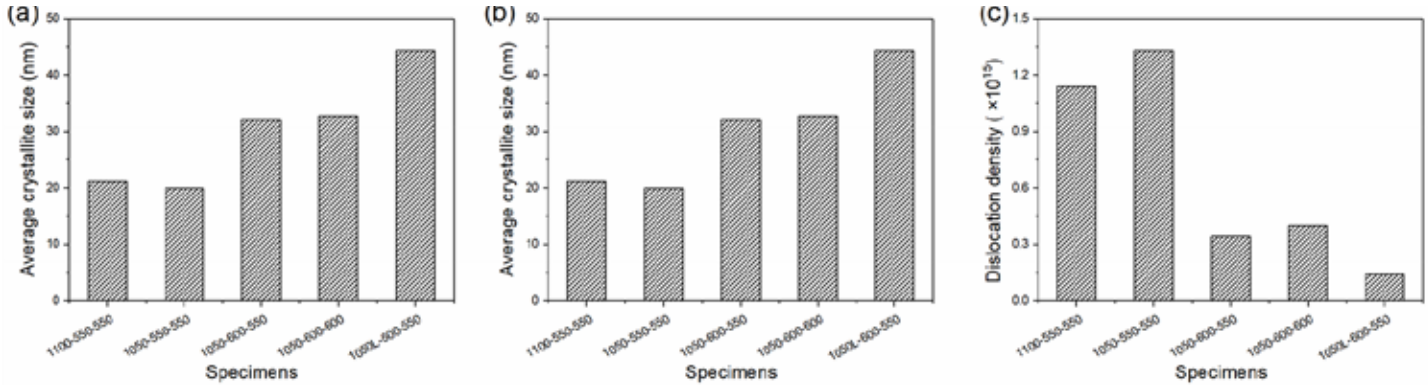

Figure 15: Average crystallite size (a), lattice strain (b), and dislocation density (c) of the heat-treated specimens.

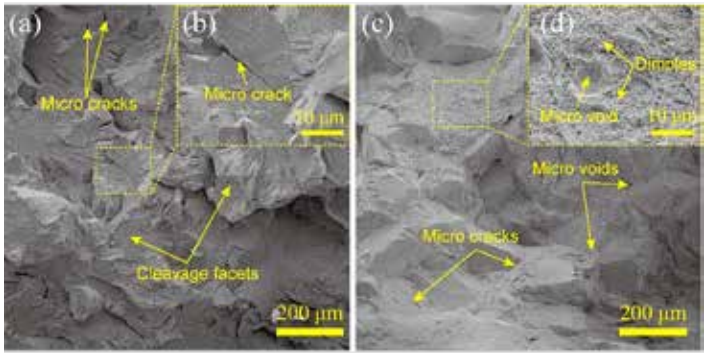

Figure 16: Fracture morphologies of (a,b) S1100-550-550 and (c,d) S1050-550-550.

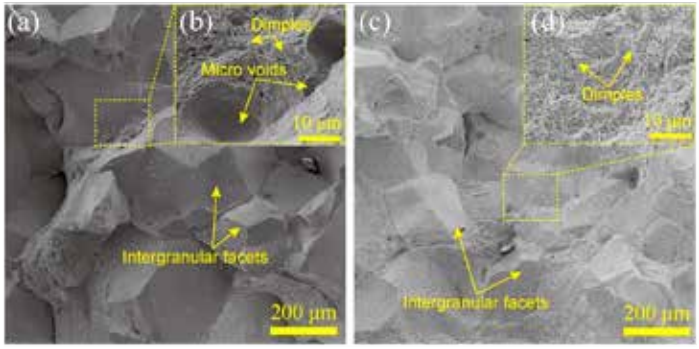

Figure 17: Fracture morphologies of (a,b) S1050-600-600 and (c,d) S1050-600-550.

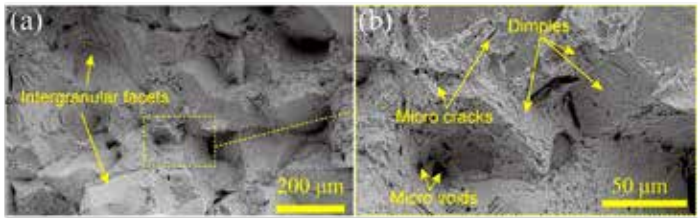

Figure 18: Fracture morphologies of S1050L-600-550. (a) Low magnification and (b) high magnification.

enhances the precipitation of carbides. To prevent coarsening of the precipitated carbides, it is necessary to lower the tempering temperature. Consequently, in S1050-600-550, the higher volume fraction and finer size of secondary carbides (Figure 11) contribute to an increase in precipitation strengthening, leading to a relatively high YS. Moreover, the reduction in lattice strain and dislocation density also enhances the ductility of the specimen. Regarding S1050L-600-550, the primary microstructures present are tempered martensite and pearlite. Consequently, the values listed for the parameters in Figure 15 for S1050L-600-550 represent a combination of the characteristics exhibited by these two structures.

3.5 Tensile Fracture

Figure 16 illustrates the tensile fracture morphologies of S1100-550-550 and S1050-550-550. As shown in Figure 16a and its detailed view in Figure 16b, the fractography of S1100-550-550 exhibits a brittle fracture model. As denoted by the yellow arrows, numerous microcracks are present on the cleavage facets, which contribute to crack propagation and fracture during tensile deformation [32,33,34]. Figure 16c,d reveals that, in addition to the intergranular fracture facets, local plastic deformation zones exist on the fracture surface. Consequently, there is a slight increase in the EL of S1050-550-550.

Figure 17 presents the fracture morphologies of S1050-600-600 and S1050-600-550, characterized by a combination of ductile and brittle fractures. The fracture surfaces exhibit a multitude of intergranular facets, suggesting brittle fracture is the predominant fracture model. However, as demonstrated in Figure 17a,c and their magnified views in Figure 17b,d, numerous fine dimples are visible, indicative of ductile fracture [34]. Therefore, S1050-600-600 and S1050-600-550 exhibit better ductility than S1050-550-550.

Figure 18 displays the fracture morphology of S1050L-600-550, comprised of dimples, cleavage facets, and micro-cracks, and demonstrating a ductile-brittle mixed mode [32,35]. Furthermore, a notable increase in the number of dimples in Figure 18a compared to Figure 17a,c suggests a growing proportion of ductile fracture in S1050L-600-550. Additionally, as shown in Figure 18b, many deep dimples are formed by the pearlite during tensile deformation, which subsequently delays crack propagation and enhances the EL of the specimen. Therefore, S1050L-600-550 exhibits a relatively high EL.

4 CONCLUSIONS

This study reveals that, by controlling processing parameters, microstructures can be tuned to achieve comprehensive mechanical properties. The key conclusions are as follows:

(1) Proper heat treatment enhances the mechanical properties of 5CrNiMoV. A balance of strength and ductility is achieved with a UTS of 1,230 MPa and an EL of 7.0% after quenching at 1,050°C, pre-tempering at 600°C, and tempering at 550°C. Furthermore, intercritical quenching at 1,050°C, pre-tempering at 600°C, and tempering at 550°C results in a higher EL of 8.2% with a UTS of 1220 MPa.

(2) Pre-tempering at 600°C and tempering at 550°C not only promotes the precipitation of carbides, but also inhibits their coarsening, effectively enhancing precipitation strengthening and contributing to a 255 MPa increase in the YS. Additionally, the decrease in the solid solution of C and Cr elements in the α-Fe matrix due to increased

carbide precipitation reduces the lattice micro-strain and dislocation density, thereby improving ductility.

(3) After intercritical quenching and tempering, the microstructure is composed of tempered martensite and pearlite. The high strength can be ascribed to the tempered martensite. The enhanced ductility is attributed to the decrease in micro-strain and dislocation density, as well as the mixed structures of tempered martensite and pearlite, which serve to hinder crack propagation during tensile deformation.

REFERENCES

[1] Huang, W.; Lei, L.; Fang, G. Microstructure evolution of hot work tool steel 5CrNiMoV throughout heating, deformation and quenching. Mater. Charact. 2020, 163, 110307.

[2] Hu, Z.; Wang, K. Evolution of Dynamic Recrystallization in 5CrNiMoV Steel during Hot Forming. Adv. Mater. Sci. Eng. 2020, 2020, 4732683.

[3] Jiang, W.; Wang, S.; Deng, Y.; Guo, X. Microstructure stability and high temperature wear behavior of an austenite aging steel coating by laser cladding. Mater. Charact. 2022, 184, 111700.]

[4] Kundu, A.; Field, D.P. Influence of microstructural heterogeneity and plastic strain on geometrically necessary dislocation structure evolution in single-phase and two-phase alloys. Mater. Charact. 2020, 170, 110690.

[5] Dobrzanski, L.; Mazurkiewicz, J.; Hajduczek, E. Effect of thermal treatment on structure of newly developed 47CrMoWVTiCeZr16-26-8 hot-work tool steel. J. Mater. Process. Technol. 2004, 157, 472–484.

[6] Wang, H.; Li, J.; Shi, C.B.; Li, J.; He, B. Evolution of Carbides in H13 Steel in Heat Treatment Process. Mater. Trans. 2017, 58, 152–156.

[7] Yu, X.-S.; Wu, C.; Shi, R.-X.; Yuan, Y.-S. Microstructural evolution and mechanical properties of 55NiCrMoV7 hot-work die steel during quenching and tempering treatments. Adv. Manuf. 2021, 9, 520–537.

[8] Zhou, Q.; Wu, X.; Shi, N.; Li, J.; Min, N. Microstructure evolution and kinetic analysis of DM hot-work die steels during tempering. Mater. Sci. Eng. A 2011, 528, 5696–5700.

[9] Zhu, J.; Zhang, Z.; Xie, J. Improving strength and ductility of H13 die steel by pre-tempering treatment and its mechanism. Mater. Mater. Sci. Eng. A 2019, 752, 101–114.

[10] Kang, C.; Liu, F.; Jiang, Z.; Zhang, H.; Ding, S. Effect of nitrogen content on solidification behaviors and morphological characteristics of the precipitates in 55Cr17Mo1VN plastic die steel. Mater. Charact. 2022, 194, 112340.

[11] Sun, J.; Wang, H.; Xu, B.; Jiang, L.; Guo, S.; Sun, X.; Yu, D.; Liu, F.; Liu, Y. Making low-alloyed steel strong and tough by designing a dual-phase layered structure. Acta Mater. 2022, 227, 117701.

[12] He, B.B.; Hu, B.; Yen, H.W.; Cheng, G.J.; Wang, Z.K.; Luo, H.W.; Huang, M.X. High dislocation density-induced large ductility in deformed and partitioned steels. Science 2017, 357, 1029–1032.

[13] Li, Y.; Yuan, G.; Li, L.; Kang, J.; Yan, F.; Du, P.; Raabe, D.; Wang, G. Ductile 2-GPa steels with hierarchical substructure. Science 2023, 379, 168–173.

[14] da Silva, E.P.; Xu, W.; Fojer, C.; Houbaert, Y.; Sietsma, J.; Petrov, R.H. Phase transformations during the decomposition of austenite below M-s in a low-carbon steel. Mater. Charact. 2014, 95, 85–93

[15] Shuai, J.; Zhao, J.; Lei, L.; Zeng, P.; Wu, X.; Sun, L. Characterization of crack propagation of Incoloy 800H by the combination of DIC and XFEM. Nucl. Eng. Des. 2020, 364, 110683.

[16] Ivanisenko, Y.; Wunderlich, R.; Valiev, R.; Fecht, H. Annealing behaviour of nanostructured carbon steel produced by severe plastic deformation. Scr. Mater. 2003, 49, 947–952.

[17] Cheng, T.; Wang, Y.; Zhao, Y.; Lv, L.; Hu, Q.; Ma, D. Effect of remelting solution heat treatment on microstructure evolution of nickel-based single crystal superalloy DD5. Mater. Charact. 2022, 192, 112186.

[18] Chen, J.; Kan, Q.; Li, Q.; Yin, H. Effects of grain size on acoustic emission of nanocrystalline superelastic NiTi shape memory alloys during fatigue crack growth. Mater. Lett. 2019, 252, 300–303.

[19] Rack, H. Role of prior austenite grain-size on the tensile ductility and fracture-toughness. Scr. Metall. 1979, 13, 577–582.

[20] Li, J.; Zhang, C.; Liu, Y. Influence of carbides on the high-temperature tempered martensite embrittlement of martensitic heat-resistant steels. Mater. Mater. Sci. Eng. A 2016, 670, 256–263.

[21] Du, N.; Liu, H.; Cao, Y.; Fu, P.; Sun, C.; Liu, H.; Li, D. In situ investigation of the fracture of primary carbides and its mechanism in M50 steel. Mater. Charact. 2022, 186, 111822

[22] Wang, K.; Guo, Z.; Sha, W.; Glicksman, M.; Rajan, K. Property predictions using microstructural modeling. Acta Mater. 2005, 53, 3395–3402. Niu, T.; Kang, Y.L.; Gu, H.W.; Yin, Y.Q.; Qiao, M.L. Precipitation Behavior and Its Strengthening Effect of X100 Pipeline Steel. J. Iron Steel Res. Int. 2010, 17, 73–78.

[23] Gladman, T. Precipitation hardening in metals. Mater. Sci. Technol. 1999, 15, 30–36.

[24] Cullity, B.D.; Stock, S.R. Elements of X-ray Diffraction, 3rd ed.; Addison-Wesley Publishing: Boston, MA, USA, 2001.

[25] Mote, V.; Purushotham, Y.; Dole, B. Williamson-Hall analysis in estimation of lattice strain in nanometer-sized ZnO particles. J. Theor. Appl. Phys. 2012, 6, 6.

[26] Sarkar, A.; Bhowmik, A.; Suwas, S. Microstructural characterization of ultra-fine-grain interstitial-free steel by X-ray diffraction line profile analysis. Appl. Phys. A 2009, 94, 943–948. Zhao, Y.; Horita, Z.; Langdon, T.; Zhu, Y. Evolution of defect structures during cold rolling of ultrafine-grained Cu and Cu-Zn alloys: Influence of stacking fault energy. Mater. Sci. Eng. A 2008, 474, 342–347.

[27] Chen, J.; Lei, L.; Fang, G. Grain-size effects on the temperature-dependent elastocaloric cooling performance of polycrystalline NiTi alloy. J. Alloys Compd. 2022, 927, 166951. Sun, W.; Xu, C.; Qiao, X.; Zheng, M.; Kamado, S.; Gao, N.; Starink, M. Evolution of microstructure and mechanical properties of an as-cast Mg-8.2Gd-3.8Y-1.0Zn-0.4Zr alloy processed by high pressure torsion. Mater. Sci. Eng. A 2017, 700, 312–320.

[28] Zhao, Y.; Bingert, J.; Topping, T.; Sun, P.; Liao, X.; Zhu, Y.; Lavernia, E. Mechanical behavior, deformation mechanism and microstructure evolutions of ultrafine-grained Al during recovery via annealing. Mater. Sci. Eng. A 2020, 772, 138706. Huang, W.; Zhong, H.; Lei, L.; Fang, G. Microstructure and mechanical properties of multi-pass forged and annealed 42CrMo steel. Mater. Sci. Eng. A 2022, 831, 142191.

[29] Chen, J.; Yin, H.; Sun, Q. Effects of grain size on fatigue crack growth behaviors of nanocrystalline superelastic NiTi shape memory alloys. Acta Mater. 2020, 195, 141–150. Wang, J.; Zhao, Y.; Zhou, W.; Zhao, Q.; Huang, S.; Zeng, W. In-situ investigation on tensile deformation and fracture behaviors of a new metastable beta titanium alloy. Mater. Sci. Eng. A 2021, 799, 140187.

[30] Chen, X.; Zhao, G.; Xu, X.; Wang, Y. Effects of heat treatment on the microstructure, texture and mechanical property anisotropy of extruded 2196 Al-Cu-Li alloy. J. Alloys Compd. 2021, 862, 158102

ABOUT THE AUTHORS

Wanhui Huang, Liping Lei, and Gang Fang are with the State Key Laboratory of Tribology in Advanced Equipment (SKLT), Department of Mechanical Engineering, Tsinghua University, Beijing.

FIND THE HEAT TREATING INFORMATION YOU NEED

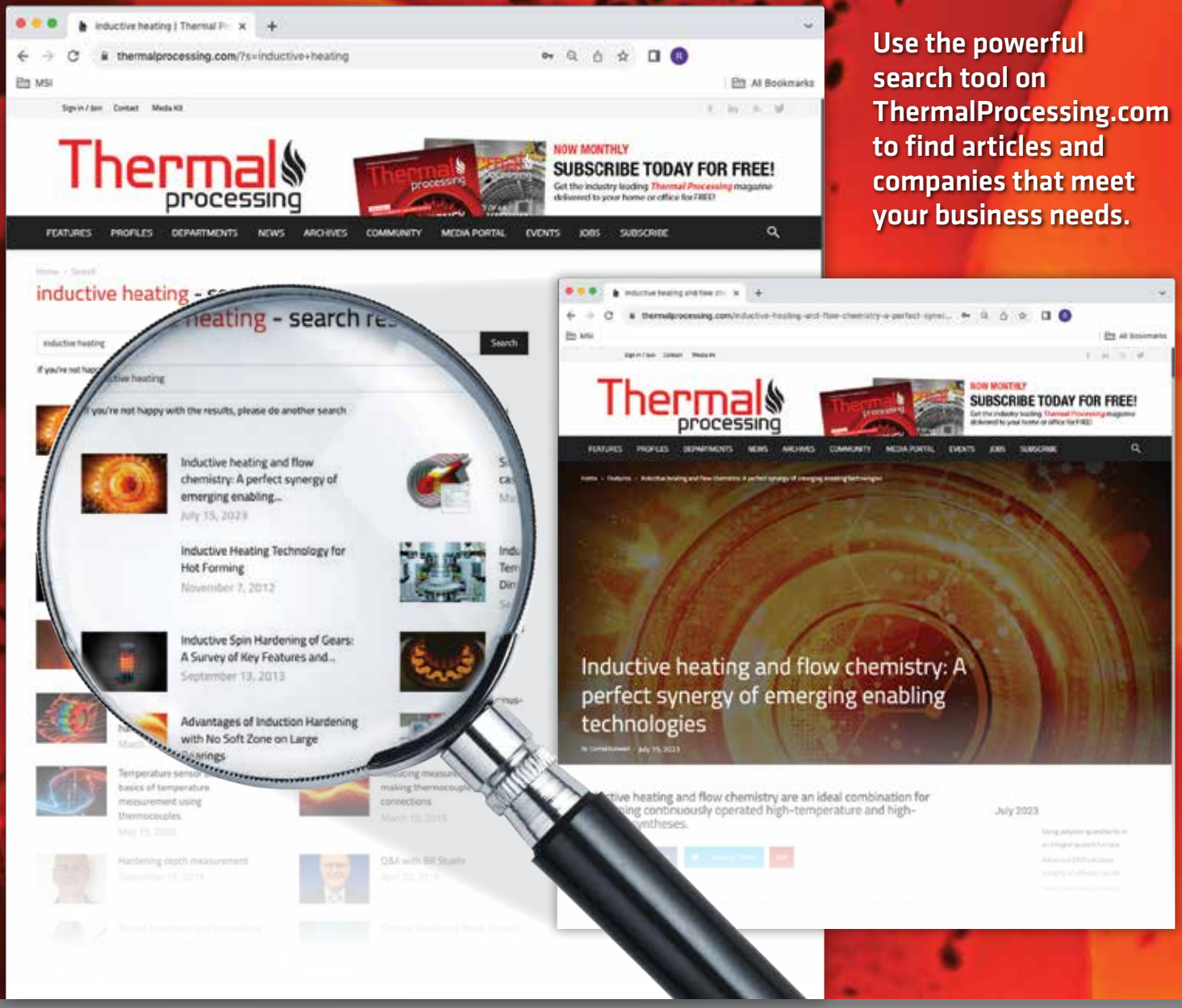

Use the powerful search tool on ThermalProcessing.com to find articles and companies that meet your business needs.

ThermalProcessing.com has a wealth of information about the heat-treat industry. And our search tool gives you access to an extensive range of articles and businesses covering all aspects of heat treating. It's there to help you find the information you need to support the success of your business.

Thermal processing

SUBSCRIBE FOR FREE

Use the QR code or go to www.thermalprocessing.com

COMPANY PROFILE ///

SCHUNK

CREATING INNOVATIVE CARBON AND GRAPHITE MATERIALS

The carbon-based fixturing created by Schunk is a lightweight alternative to alloy fixturing. (Courtesy: Schunk)

As a leading supplier in the field of carbon technology, Schunk develops and produces customized solutions for demanding industrial applications worldwide.

By KENNETH CARTER, Thermal Processing editor

When it comes to heat treating, carbon often plays a vital part of almost any process. That's particularly true when it comes to various parts heat treated in vacuum furnaces.

Carbon is a useful material because of its wide range of properties — mechanical, electrical, and thermal. Schunk has a long history in the U.S. of providing electrical and mechanical components, and now they are adding a focus to the thermal side of the carbon equation.

"Out of our location here in the U.S., we focus on fixturing or carrier trays to heat treat metal parts in vacuum furnaces," said Brett Swenson, Strategic Business Area Manager, North & Central America — Thermal Carbon sales at Schunk. "In an open-air atmosphere, carbon-fiber fixturing will oxidize due to the presence of oxygen, but in a controlled atmosphere, like in a vacuum furnace, it can be an excellent alternative to alloy fixturing. We've assembled a team of engineers dedicated to these materials here in the U.S. And over the last two years we have built up our production capabilities, and so we now have a one-stop solution now for our customers where they can come to us, and we can design and build custom-based fixturing for them."

CARBON-BASED FIXTURING

The carbon-based fixturing created by Schunk is a lightweight alternative to alloy fixturing, according to Swenson.

"This means you can run more parts per load," he said. "Carbon fiber also heats up and cools down quicker than alloy, allowing for reduced process times. A benefit is that it holds its form over repeated cycles, compared to alloys that warp over time. This means increased repeatability, and in a world where a lot of processes are changing over to being automated, repeatability is key. We also offer all of the relining components and graphite insulation for vacuum furnaces, as well as carbon fiber temperature uniformity fixtures."

As Schunk remains on the cutting edge of technology, it has allowed the company to enter the aerospace and defense fields, as well as renewable energy, according to Swenson.

"We develop advanced materials for large-scale battery storage applications and collaborate with transit authorities nationwide to electrify buses as they transition away from diesel, he said. "We also supply materials to companies pioneering clean carbon black and clean hydrogen production, as well as those manufacturing graphite for EV batteries. You have these new technologies that are helping drive sustainability and improve the environment, and we see our responsibility there to help supply materials for those types of markets."

DECADES OF CHANGE

To that end, Schunk has been and continues to be forward thinking, according to Swenson.

"We've been able to keep up with a lot of changes over the decades," he said. "We started as a materials company, but we realized there was an opportunity to get into the machine side as well. Globally, the Schunk Group is now split into two divisions: Materials and Machines. One of the strengths of Schunk is the diversity of its portfolio. The location I am based out of in Wisconsin specializes in the manufacturing of carbon-based products. But we have another location that focuses on technical ceramics and graphite used in the production of semiconductors."

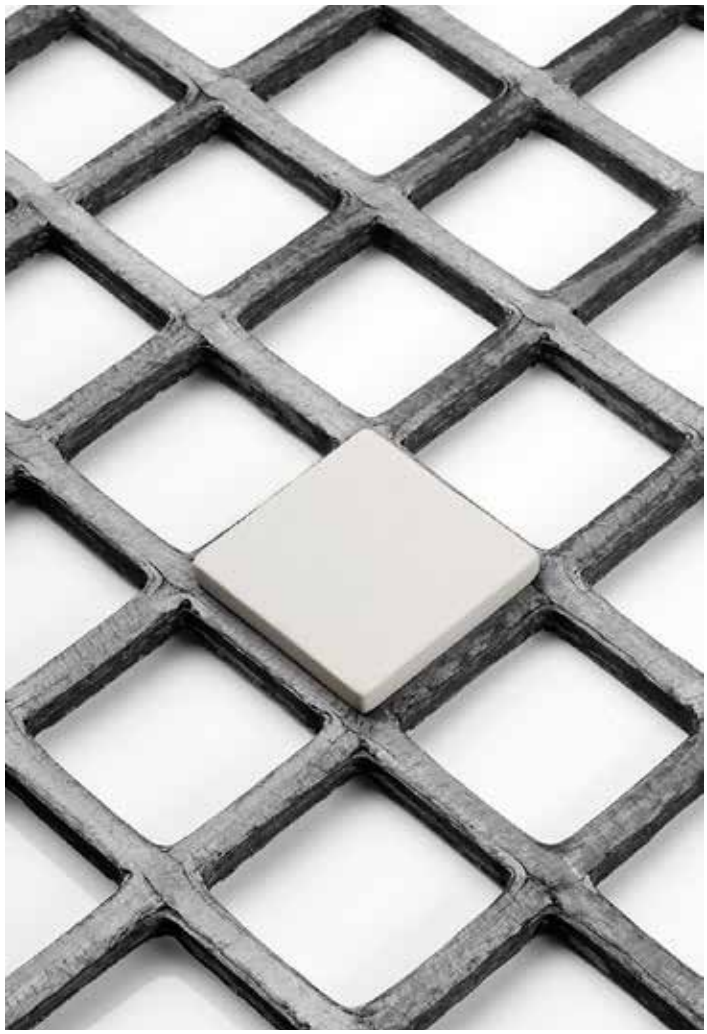

Schunk developed a product called the UniGrid, a single carbon fiber that's woven into a grid pattern. (Courtesy: Schunk)

Schunk's ability to diversify has kept it competitive as well as innovative, according to Swenson.

"We acquired a company that makes machines that cut glass for optical lenses," he said. "We also have a company that builds ultrasonic welding machines. By being able to diversify the different products that we can offer, we've been able to evolve as a company. We've seen a lot of crossover between those types of industries and markets as well.

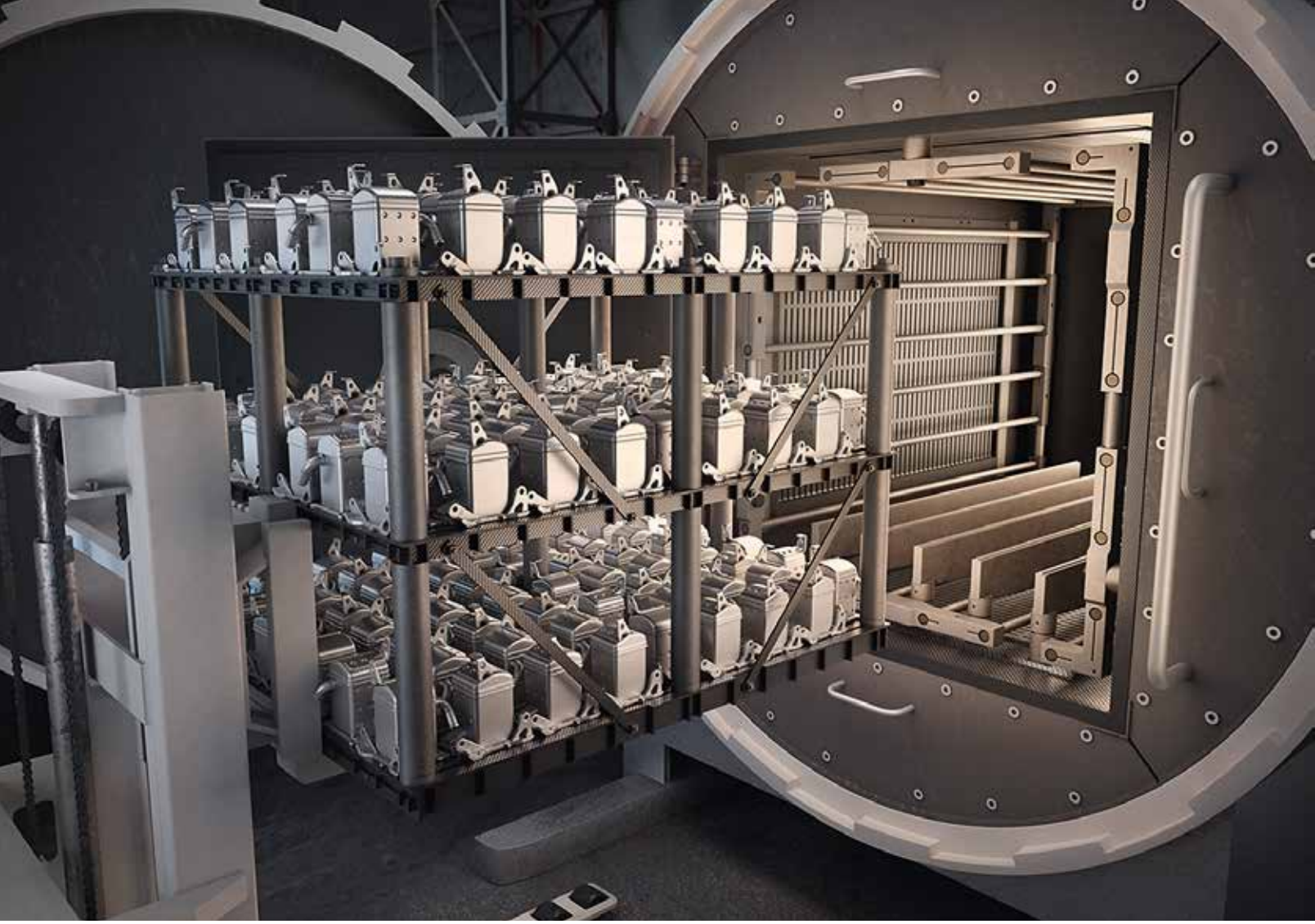

Schunk focuses on fixturing or carrier trays to heat treat metal parts in vacuum furnaces. (Courtesy: Schunk)

We might be in a heat-treat facility and see that maybe they're using a product that we could offer a solution using our electrical carbon for or maybe use the mechanical carbon for. There's a lot of opportunity there, and I feel like we're in a good position to capitalize on that."

CUSTOMER FOCUSED

Innovation isn't the main ingredient to Schunk's success. Focusing on the customer is just as important, according to Swenson.

"We're customer first; we are really idea driven," he said. "A lot of the investment that we have goes into research and development. We like to break into new markets. We like being on the cutting edge of different technologies, but if we do something, we're not going to do it unless we know that we can do it well. We take risks, but it's always a calculated risk. That approach sets us up for strong, long-term solutions and stability. That's how we view our customers as well. We don't want to just sell the customer something and then walk away. We view our customers as partners, and so we want to continue to support them after the sale is made and continue to collaborate with them on future projects."

That element of working with its customers is key to Schunk's longevity, according to Swenson.

"We want to work with our customers," he said. "We view them as partners, so there's a lot of collaboration there. We may not be experts in the different processes that our customers are doing, but we know that we can supply materials to help improve their processes. We ask a lot of questions. We try to learn what their processes are.

"We want to work with our customers. We view them as partners, so there's a lot of collaboration there."

What's interesting about carbon is that often, when you're using it, you can identify potential issues in a customer's process because of the way the carbon interacts or appears at the end of that process. We approach it like a fact-finding mission, and we do a lot of problem solving with them when they bring us their issues. We want to provide a solution that's practical for them and something that will be a long-lasting solution for them."

MORE THAN A CENTURY OF SOLUTIONS

Schunk has been in business for more than a century, so it stands to reason that the company has received many accolades and been at the forefront of innovative products. For example, Schunk has won many supplier quality awards with large OEMs in the automotive and aerospace industries.

On the heat-treat side, Schunk developed a product called the UniGrid, according to Swenson.

"it's a single carbon fiber that's woven into a grid pattern, and then we add a carbon-based resin to hold it all together," he said. "It's a two-foot by three-foot grid, and, depending on how it's positioned, it can hold up to a couple hundred pounds. It's used as an off-the-shelf option as a carrier tray on the heat-treating side of things. We started selling those to customers 15 years ago, and they're still using the same ones today. It's a long-lasting product. What we aim to do as a company is make high-end, long-lasting products."

UNIQUE HISTORY

Schunk's innovative solutions are surely enough to keep it high on the industrial map, but perhaps just as interesting is the way the company is structured.

Schunk was founded in 1913 by Ludwig Schunk where it started as a carbon brush company. Over the decades, Schunk continued to acquire other carbon-based manufacturers, and in the 1970s, it moved to the U.S., according to Swenson.

"We've been in the U.S. for about 40 years with the carbon-manufacturing side, and that's the facility that I work at now, which is a little bit north of Milwaukee," he said. "We're a materials supplier. Schunk is separated into two different sides: There's the materials side, which is all carbon-based materials, and then there's the machine side."

When Ludwig Schunk died, he had no one to leave the company to, so instead of leaving it to a child or another owner, he created a foundation that's still set up that way today, according to Swenson.

"The Schunk Group has many characteristics of an employee-owned business, as it's set up as a foundation, and has a board that manages the foundation," he said. "All of the companies, which are in 26 different countries — and there are over a hundred companies with over 10,000 employees — they all report back to the Schunk Group. All of the profits go back to the group, and they reinvest all of that money into the employees and into the company. Whether that's R&D, buildings, merger acquisitions, or other initiatives, it all gets put back into the company. This structure creates a real stability and long-term strength."

And if that sounds unique, it is, often to the astonishment of others, according to Swenson.

High-temp CFC. (Courtesy: Schunk)

"We like telling that story, because every time we tell the story, that's kind of the reaction that we get — it's a very unique setup," he said. "We're not publicly traded in any country. We don't have to answer to a board of directors. We have a nice setup that creates a good culture for the employees."

EYE ON THE FUTURE

That company structure has been a benefit to the diversity and innovation that Schunk has been successful with, and with its foot already into the next century, Swenson said challenges will be met with the same expertise and enthusiasm that it always has.

"Obviously, politics influence the future, and they'll always influence it," he said. "Every election cycle you'll see a change, but right now, we see a lot of manufacturing being brought into the U.S. We see the manufacturing sector growing in the U.S., and we're trying to position ourselves to be able to support that growth and be a part of that growth."

As an example of that, Swenson pointed out that, up until about two years ago, Schunk didn't have any production capabilities in the U.S. for the heat-treat side of the business.

"We've had our production facility for 40 years, but it supported our other business units," he said. "Now we've brought it in for the thermal carbon side. The whole idea is that we're trying to keep up with where we see the industry going. We feel that we can be a good local partner to help supply manufacturers who are looking to create locally made products. From an engineering and fabrication standpoint, we think we'll be in a good spot to be able to do that."

MORE INFO www.schunk-group.com

MARKETPLACE ///

Manufacturing excellence through quality, integration, materials, maintenance, education, and speed.

Contact **Thermal Processing** at 800-366-2185 to feature your business in the Marketplace.

ADVERTISER INDEX ///

MICHAEL ZULAUF /// PRODUCT MANAGER /// WEILER ABRASIVES

"Our (Tiger Mill Scale wheel) lasts longer than the competition because it incorporates a zirconia-based grinding wheel formulation."

What is heavy mill scale, and what problems can it cause?
Mill scale is a thin, flaky layer of bluish iron oxides that forms on the surface of steel during the hot rolling process. Mill scale primarily consists of three different iron oxide layers: wüstite, magnetite, and hematite. Wüstite is the innermost layer, closest to the steel substrate. Magnetite is the middle layer. It's more stable and denser. Hematite is the outermost layer, comprising a thin, brittle crust. It's a naturally occurring byproduct of the hot rolling process. It ranges from about four-thousandths of an inch up to several millimeters thick. It can be thick and brittle, non-uniform or uniform, and it creates a barrier to effective welding and surface preparation.

What causes this on hot-rolled carbon steel?
When the steel is heated to a high temperature in a furnace and then rolled into sheets, the surface reacts with oxygen in the air, producing the characteristic coating. The chemistry of the metal, as well as the moisture content and chemistry of the environment, are all variables that will affect the types and amount of scale that will form.

What has Weiler Abrasives done to address this problem?
We've developed a solution specifically for this. It is called the Tiger Mill Scale wheel. We've gone through a lot of customer requests, customer feedback, and field trials, to get the product we have now.

What makes the Tiger Mill Scale wheel superior to what already exists in the market?
There are very few options out there to start with. Operators will come up with all kinds of cumbersome ways to get the job done. But our formulation lasts longer than the competition because it incorporates a zirconia-based grinding wheel formulation, as opposed to the very few others out there that are more of a softer unitized formulation. We've implemented a studded pattern on a Type 29 wheel for easy access to a larger, flatter surface, which minimizes guard interference and the potential to gouge the workpiece. The studded pattern on the surface of the wheel resists loading and allows built-up flakes to shed, providing a smaller localized surface area that breaks through the thick scale.

How was it dealt with before this type of technology existed?
There are other more cumbersome options out there. Manual grinding isn't the only way to remove mill scale. There are higher cost, more complex ways to remove it. Flame cleaning is quick, but it risks heat distortion and often doesn't fully remove the scale. There is abrasive blasting, which is fast and effective, but it's very dusty, and it's very high in consumable costs. There's chemical pickling, which is thorough, but it's very slow, taking about 24 hours. It's hazardous and it's waste-heavy. And then, there's manual grinding, which is precise, but can be labor-intensive, slow for large areas and most abrasives would tend to clog and stop working. That's why we came up with this option: to make manual mechanical grinding a viable and efficient method.

What types of industries see heavy mill scale removal as a critical operation, and why is that?
It's critical in construction, manufacturing and fabrication, automotive and heavy equipment, transportation, oil and gas, natural energy — really anywhere hot-rolled steel is used in heavy structural fabrication.

As I mentioned, removing mill scale is critical to ensure proper weld penetration. Our wheel quickly and easily removes mill scale without gouging or removing too much base material. The operator can move quickly over the surface without dwelling or excessive force, and the resulting steel surface is free of scale and ready to accept a weld. When the surface isn't clean, the mill scale itself causes porosity, lack of fusion, weld defects, and reduces weld quality. It creates barriers to effective welding and surface prep. It acts as an insulator, causing arc instability and poor heat transfer while you're welding. It leads to a weak fusion and compromised structural integrity of the weld itself. And ultimately, it can end in weld failures, costly rework, and potential catastrophic failures.

What has been the market response to the Tiger Mill Scale wheel?
It's been excellent. The operators who have tried it ask how fast they can get it in their shop. Most of the work we've been doing was ahead of the launch, which was only a few weeks ago, so we can't get it to them fast enough, which is always a good thing.

MORE INFO www.weilerabrasives.com


YOU'VE GOT THE PRODUCTS.
YOU'VE GOT THE SERVICES.
NOW, LET US SHARE YOUR STORY.
Thermal Processing wants to make sure the best possible audience knows your company. Through our print, online, and social media presence, our experienced staff can get your message to an industry that wants to know what you can do.
To learn more, contact our sales team at sales@thermalprocessing.com or call 800.366.2185
Thermal processing

Vacuum Heat Treating & Brazing Services

Annealing • Aging • Carburizing • Nitriding • Stress Relieving • Degassing • Brazing • Harden and Temper
Sintering • Solution Treat and Age (STA) • Homogenizing • Creep Forming • Hydriding / Dehydriding

Solve your toughest thermal processing challenges by utilizing our brain-trust of metallurgists, chemists and engineers.

- Over 90 vacuum furnaces – lab-sized to 48 feet long
- Argon, nitrogen and helium quenching up to 20 bar
- Operating range of -320°F to +3,600°F
- On-site metallurgical testing lab
- 24/7 Operations

SOLAR ATMOSPHERES

1-855-WE-HEAT-IT
solaratm.com

Nadcap Administered by PRI ACCREDITED HEAT TREATING NONDESTRUCTIVE TESTING

ISO9001 AS9100 Registered

MedAccred Heat Treating

Eastern PA • Western PA • California • South Carolina • Michigan • San Diego